U-Pb geochronological data for intrusive rocks near the Schaft Creek and Galore Creek deposits (southern Telegraph Creek area, NTS 104G), northwestern British Columbia

Leif Bailey, Rachel Kim, Mike Takaichi, James Logan,
Jim Crowley, Richard Friedman, Corey Wall,
Bram I. van Straaten, Roddy Campbell

British Columbia
Ministry of Mining and Critical Minerals

GeoFile 2025-14

Ministry of Mining and Critical Minerals
Responsible Mining and Competitiveness Division
British Columbia Geological Survey

Recommended citation: Bailey, L., Kim, R., Takaichi, M., Logan, J., Crowley, J., Friedman, R., Wall, C., van Straaten, B.I., and Campbell, R., 2025. U-Pb geochronological data for intrusive rocks near the Schaft Creek and Galore Creek deposits (southern Telegraph Creek area, NTS 104G), northwestern British Columbia. British Columbia Ministry of Mining and Critical Minerals, British Columbia Geological Survey GeoFile 2025-14, 16 p.

Front cover:
Plagioclase-megacrystic diorite of the Hickman pluton, Stikine plutonic suite (Late Triassic) sampled for U-Pb zircon geochronology (sample LB-14-069). **Photo by Leif Bailey.**

Back cover:
Cathodoluminescence image of zircon grains from the Pereleshin pluton, Cone Mountain plutonic suite (late Early Jurassic; sample RK23-034). **Photo by Corey Wall.**

Ministry of
Mining and
Critical Minerals

U-Pb geochronological data for intrusive rocks near the Schaft Creek and Galore Creek deposits (southern Telegraph Creek area, NTS 104G), northwestern British Columbia

Leif Bailey
Rachel Kim
Mike Takaichi
James Logan
Jim Crowley
Richard Friedman
Corey Wall
Bram I. van Straaten
Roddy Campbell

Ministry of Mining and Critical Minerals
British Columbia Geological Survey
GeoFile 2025-14

U-Pb geochronological data for intrusive rocks near the Schaft Creek and Galore Creek deposits (southern Telegraph Creek area, NTS 104G), northwestern British Columbia

Leif Bailey[1,2], Rachel Kim[2], Mike Takaichi[1], James Logan[3], Jim Crowley[4], Richard Friedman[5], Corey Wall[5], Bram I. van Straaten[6,a], Roddy Campbell[6]

[1] Teck Resources Limited, Vancouver, BC, V6C 0B3
[2] Galore Creek Mining Corporation, Vancouver, BC, V6C 0B3
[3] JLoGeologic, Victoria, BC, V8L 5Z9
[4] Isotope Geology Laboratory, Department of Geosciences, Boise State University, Boise, ID, 83725, USA
[5] Pacific Centre for Isotopic and Geochemical Research, Department of Earth, Ocean and Atmospheric Sciences, The University of British Columbia, Vancouver, BC, V6T 1Z4
[6] British Columbia Geological Survey, Ministry of Mining and Critical Minerals, Victoria, BC, V8W 9N3, Canada

[a] Corresponding author: Bram.vanStraaten@gov.bc.ca

Recommended citation: Bailey, L., Kim, R., Takaichi, M., Logan, J., Crowley, J., Friedman, R., Wall, C., van Straaten, B.I., and Campbell, R., 2025. U-Pb geochronological data for intrusive rocks near the Schaft Creek and Galore Creek deposits (southern Telegraph Creek area, NTS 104G), northwestern British Columbia. British Columbia Ministry of Mining and Critical Minerals, British Columbia Geological Survey GeoFile 2025-14, 16 p.

Abstract
This release provides U-Pb geochronology data for 19 intrusive rock samples from northwestern British Columbia. Samples were collected between 2005-2023 by Teck Resources Limited, Galore Creek Mining Corporation and the British Columbia Geological Survey from Late Triassic to Cretaceous intrusive rocks within the Stikine terrane. The dataset can be used to better understand the magmatic evolution of the Stikine terrane, particularly as it relates to the Schaft Creek and Galore Creek porphyry deposits.

Keywords: Geochronology, U-Pb, zircon, CA-TIMS, LA-ICPMS, ID-TIMS, Schaft Creek, Galore Creek, porphyry Cu-Au-Mo-Ag deposit, intrusive rocks, plutonic rocks, Stikine terrane, Triassic, Jurassic, Cretaceous, Stikine plutonic suite, Hickman batholith, Hickman pluton, Nightout pluton, Cone Mountain plutonic suite, Pereleshin pluton, Scud River stock, upper Hazelton Group, Three Sisters plutonic suite, Yehiniko pluton

1. Introduction

Herein we present U-Pb zircon geochronologic results from 19 intrusive rock samples collected between 2005-2023 (Fig. 1; Table 1). In Appendix 1 (BCGS_GF2025-14.zip) are folders with analytical data and zircon images. For detailed geological descriptions of the intrusive rocks, the reader is referred to Logan and Koyanagi (1994), Brown et al. (1996), Campbell and van Straaten (2025), and references therein. The following details the analytical methods we used, summarizes sample descriptions, and presents how we interpret the derived ages.

2. Analytical methods

2.1. 2005 sample

One sample collected in 2005 was analyzed at the Geochronology Laboratory of the University of British Columbia (UBC), Vancouver, BC using ID-TIMS.

2.1.1. ID-TIMS methods

Zircons were separated from 1-50 kg samples using conventional crushing, grinding, and Wilfley table techniques, followed by final concentration using heavy liquids and magnetic separations. Mineral fractions were selected for analysis based on grain morphology, quality, size, and magnetic susceptibility. All zircon fractions were air abraded before dissolution to minimize the effects of post-crystallization Pb-loss using the technique of Krogh (1982). All geochemical separations and mass spectrometry were done following methods described in Mortensen et al. (1995).

Selected zircons were dissolved in concentrated HF and HNO_3 in the presence of a mixed $^{233-235}U$-^{205}Pb isotopic tracer. The zircon fractions were dissolved in Teflon microcapsules within Parr bombs for 40 h at 240°C. The HF solution was evaporated, and fluorides were dissolved in 3.1 N HCl in Parr

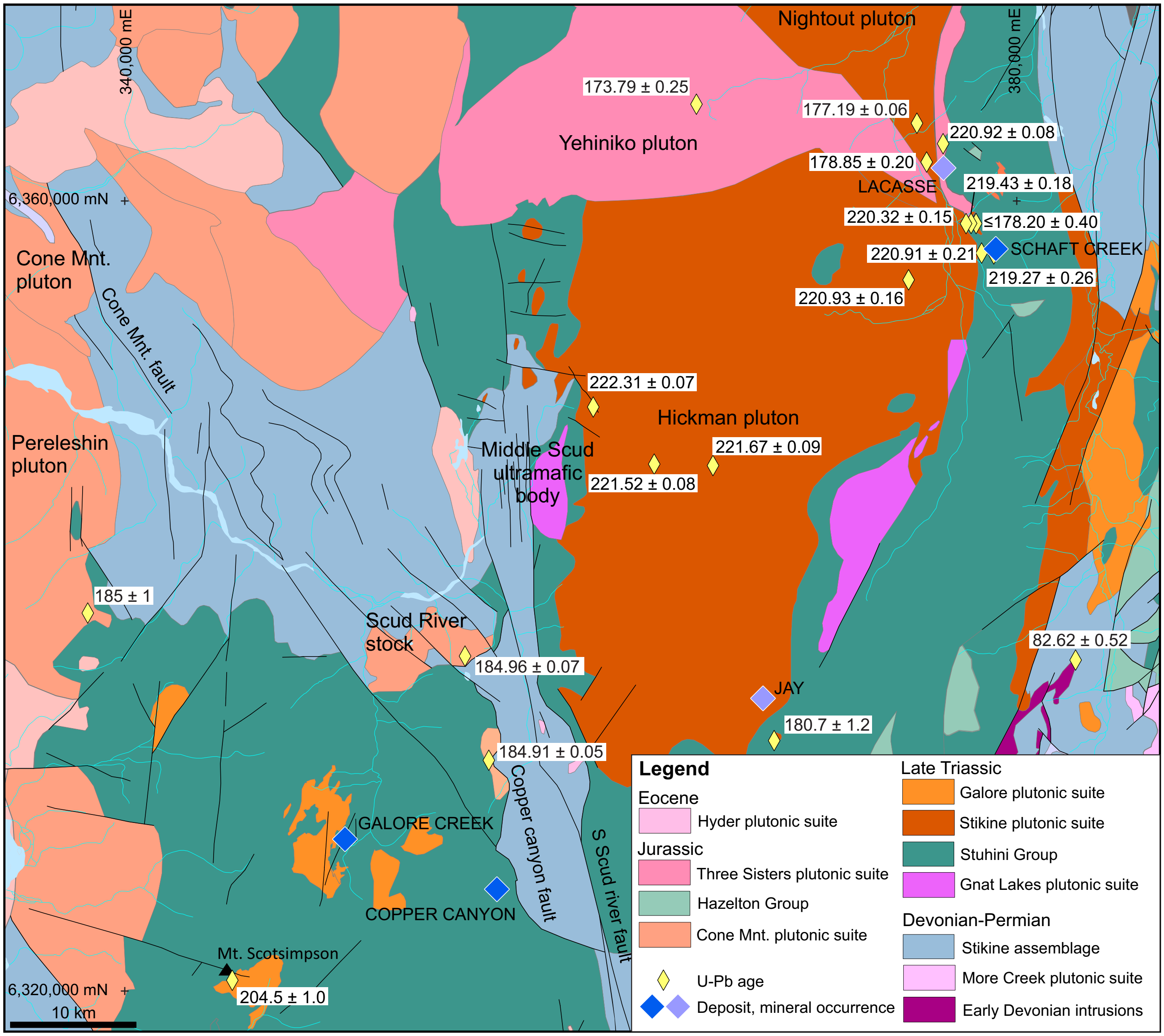

Fig.1. Bedrock geology near the Schaft Creek and Galore Creek deposits, southern Telegraph Creek area (NTS 104G), with geochronology sample locations. Modified after Campbell and van Straaten (2025).

bombs for 12 h at 210°C. HF was evaporated, and fluorides were dissolved in 6.2 N HCl on a hot plate for 24 h. This solution was evaporated to dryness, and chlorides were dissolved on the hot plate for 24 h. Separation and purification of Pb and U from zircon fractions employed ion exchange column techniques, modified slightly from those described by Parrish et al. (1987). Pb and U were eluted separately and loaded together on a single Re filament using a phosphoric acid-silica gel emitter. Isotopic ratios were measured using a modified single collector VG-54R thermal ionization mass spectrometer equipped with a Daly photomultiplier. Most measurements were in peak-switching mode on the Daly detector. U and Pb analytical blanks were in the range of 1 pg and 1-5 pg, respectively, during this study. U fractionation was determined directly on individual runs using the $^{233\text{-}235}U$ tracer. Pb isotopic ratios were corrected for a fractionation of 0.12%/amu and 0.35%/amu for Faraday and Daly runs, respectively, based on replicate analyses of the NBS-981 Pb standard and the values recommended by Todt et al. (1984). All analytical errors were propagated through the entire age calculation using the technique of Roddick (1987). Concordia intercept ages and associated errors were calculated using a modified version of the York-II-regression model (wherein the York-II errors are multiplied by the square root of the MSWD, when greater than 1) and the algorithm of Ludwig (1980). Errors for Pb/U and Pb/Pb ages are quoted at 2 sigma level. Results are shown in folder '2005_UBC' of Appendix 1.

2.2. 2013 samples

Seven samples collected in 2013 were analyzed at the Pacific Centre for Isotopic and Geochemical Research (PCIGR) at the University of British Columbia, Vancouver, BC by CA-TIMS.

Table 1. U-Pb zircon geochronological results for 19 samples from the southern Telegraph Creek area, including the Schaft Creek and Galore Creek deposits. Coordinates in UTM Zone 9 north, NAD83. All ages are based on weighted mean $^{206}Pb/^{238}U$ dates. Mineral abbreviations after Kretz (1983). Equigr.: equigranular, porph.: porphyritic, SC: Schaft Creek, * includes LA-ICPMS reconnaissance. See van Straaten (2024), Campbell and van Straaten (2025) for unit codes, and Jutras and Bailey (2016), Erbalaban (2023) for logging codes. GCMC = Galore Creek Mining Corporation; Teck = Teck Resources Limited.

Sample ID	Year taken	Project	Area	UTM E	UTM N	Age ± error	Analytical method (lab)	Lithology	Unit
RK23-117	2023	Galore (GCMC)	Mess Creek	383214	6341909	82.62 ±0.52	LA-ICPMS (PCIGR)	Equigr. Px-Bt diorite	LKd
SCK-2013-MLT-012Y	2013	Schaft (Teck)	Yehiniko pluton	366249	6366048	173.79 ±0.25	CA-TIMS (PCIGR)	Hbl-bearing Bt syenogranite	MJTgg
GJ-14-001	2014	Schaft (Teck)	SC: LaCasse zone	377766	6364379	177.19 ±0.06	CA-TIMS (BSU)	Qtz syenite dike	MJTgg or EMJhf
2010CF401-140m	2013	Schaft (Teck)	SC: Paramount zone	379414	6360801	≤178.20 ±0.40	CA-TIMS (PCIGR)	Px-Pl porphyry dike	EMJhm
SCK14-SH836	2014	Schaft (Teck)	SC: LaCasse zone	377990	6363528	178.85 ±0.20	CA-TIMS* (BSU)	Flow-banded felsic dike	EMJhf
RK23-037	2023	Galore (GCMC)	S of Hickman pluton	370178	6338782	180.7 ±1.2	LA-ICPMS (PCIGR)	Porph. Bt Qtz monzonite to granodiorite	EMJhf
19JLo25-344	2019	Galore (GCMC)	N of Copper canyon	357741	6338367	184.91 ±0.05	CA-TIMS (BSU)	Equigr. Hbl Qtz monzonite	EJCdqm
LB-14-218	2014	Schaft (Teck)	Scud River stock	356851	6342869	184.96 ±0.07	CA-TIMS* (BSU)	Porph. Qtz monzodiorite to Qtz monzonite	EJCdqm
RK23-034	2023	Galore (GCMC)	Pereleshin pluton	340634	6345239	185 ±1	LA-ICPMS (PCIGR)	Equigr. Bt Qtz monzonite	EJCdqm
ABA05-46-369	2005	Galore (BCGS)	E of Mt. Scotsimpson	346290	6329260	204.5 ±1.0	ID-TIMS (UBC)	Equigr. Hbl-bearing Bt-Cpx syenite	LTrGdm
H69CH046-249.8m	2013	Schaft (Teck)	SC: Liard zone	380196	6359465	219.27 ±0.26	CA-TIMS (PCIGR)	Crowded Qtz-Hbl(?)-Bt-Pl porphyry dike	LTrSh (sPOR)
P69CH02-32m	2013	Schaft (Teck)	SC: Paramount zone	379257	6360805	219.43 ±0.18	CA-TIMS (PCIGR)	Moderately crowded Hbl-Pl porphyry dike	LTrSh (sPOR)
08CF364-31.7m	2013	Schaft (Teck)	SC: Paramount zone	379041	6360803	220.32 ±0.15	CA-TIMS (PCIGR)	Equigr. Hbl(?) granodiorite	LTrSgd (GRD)
08CF326-76m *(34.4-81m)*	2013	Schaft (Teck)	SC: West Breccia zone	379672	6359517	220.91 ±0.21	CA-TIMS (PCIGR)	Hbl Qtz monzodiorite	LTrSgd (QMZ)
GJ-14-002	2014	Schaft (Teck)	SC: LaCasse zone	378149	6364025	220.92 ±0.08	CA-TIMS* (BSU)	Equigr. granodiorite	LTrSgd (GRD)
SCK-2013-MLT-011HA	2013	Schaft (Teck)	Hickman pluton	376498	6358462	220.93 ±0.16	CA-TIMS (PCIGR)	Equigr. Bt-Hbl granodiorite	LTrSgd
LB-14-132	2014	Schaft (Teck)	Hickman pluton	365297	6350886	221.52 ±0.08	CA-TIMS (BSU)	Equigr. Bt-Hbl granodiorite	LTrSgd
LB-14-227	2014	Schaft (Teck)	Hickman pluton	367827	6350741	221.67 ±0.09	CA-TIMS* (BSU)	Syenite to Qtz monzonite	LTrSdqm?
LB-14-069	2014	Schaft (Teck)	Hickman pluton	362752	6353429	222.31 ±0.07	CA-TIMS (BSU)	Pl-megacrystic Hbl diorite	LTrSd.tm

2.2.1. CA-TIMS methods

The CA-TIMS procedures described here are modified from Mundil et al. (2004), Mattinson (2005), and Scoates and Friedman (2008). After rock samples underwent standard mineral separation procedures, zircons were handpicked in alcohol. The clearest, crack- and inclusion-free grains were selected, photographed, and then annealed in quartz glass crucibles at 900°C for 60 hours. Annealed grains were transferred into 3.5 mL PFA screwtop beakers, ultrapure HF (up to 50% strength, 500 µL) and HNO_3 (up to 14 N, 50 µL) were added and caps were closed finger tight. The beakers were placed in 125 mL PTFE liners (up to four per liner) and about 2 mL HF and 0.2 mL HNO_3 of the same strength as acid within beakers containing samples were added to the liners. The liners were then slid into stainless steel Parr high pressure dissolution devices, which were sealed and brought up to a maximum of 200°C for 8-16 hours (typically 175°C for 12 hours). Beakers were removed from liners and zircon was separated from leachate. Zircons were rinsed with >18 MΩ.cm water and subboiled acetone. Then 2 mL of subboiled 6N HCl was added, and beakers were set on a hotplate at 80°-130°C for 30 minutes and again rinsed with water and acetone. Masses were estimated from the dimensions (volumes) of grains. Single grains were transferred into clean 300 µL PFA microcapsules (crucibles), and 50 µL 50% HF and 5 µL 14 N HNO_3 were added. Each was spiked with a $^{233-235}U$-^{205}Pb tracer solution (EARTHTIME ET535), capped and again placed in a Parr liner (8-15 microcapsules per liner). HF and nitric acids in a 10:1 ratio, respectively, were added to the liner, which was then placed in Parr high pressure device and dissolution was achieved at 240°C for 40 hours. The resulting solutions were dried on a hotplate at 130°C, 50 µL 6N HCl was added to microcapsules and fluorides were dissolved in high pressure Parr devices for 12 hours at 210°C. HCl solutions were transferred into clean 7 mL PFA beakers and dried with 2 µL of 0.5 N H_3PO_4. Samples were loaded onto degassed, zone-refined Re filaments in 2 µL of silicic acid emitter (Gerstenberger and Haase, 1997).

Isotopic ratios were measured using a modified single collector VG-54R or 354S (with Sector 54 electronics) thermal ionization mass spectrometer equipped with analogue Daly photomultipliers. Analytical blanks were 0.2 pg for U and up to 1 pg for Pb. U fractionation was determined directly on individual runs using the EARTHTIME ET535 mixed $^{233-235}U$-^{205}Pb isotopic tracer and Pb isotopic ratios were corrected for fractionation of 0.25%/amu, based on replicate analyses of NBS-982 reference material and the values recommended by Thirlwall (2000). Data reduction employed the Excel-based program of Schmitz and Schoene (2007). Standard concordia diagrams were constructed and weighted averages calculated with Isoplot (Ludwig, 2003). Unless otherwise noted all errors are quoted at the 2 sigma or 95% confidence level. Isotopic dates are calculated with the decay constants $\lambda_{238} = 1.55125 \times 10^{-10}$ and $\lambda_{235} = 9.8485 \times 10^{-10}$ (Jaffe et al., 1971). EARTHTIME U-Pb synthetic solutions were analysed on an on-going basis to monitor the accuracy of results. Results are given in folder '2013_PCIGR' of Appendix 1.

2.3. 2014 and 2019 samples

Seven samples collected in 2014, and one sample collected in 2019 were analyzed at Boise State University (BSU) in Boise, Idaho, USA using LA-ICPMS and CA-TIMS.

2.3.1. LA-ICPMS methods

Zircon grains were separated from rocks using standard techniques and annealed at 900°C for 60 hours in a muffle furnace. They were mounted in epoxy and polished until their centers were exposed. Cathodoluminescence (CL) images from seven samples were obtained with a JEOL JSM-1300 scanning electron microscope and Gatan MiniCL. Zircons from four samples were analyzed by laser ablation inductively coupled plasma mass spectrometry (LA-ICPMS) using a ThermoElectron X-Series II quadrupole ICPMS and New Wave Research UP-213 Nd:YAG UV (213 nm) laser ablation system. In-house analytical protocols, standard materials, and data reduction software were used for acquisition and calibration of U-Pb dates and a suite of high field strength elements (HFSE) and rare earth elements (REE). The zircons were ablated with a laser spot of 25 µm wide using fluence and pulse rates of 5 J/cm^2 and 10 Hz, respectively, during a 45 second analysis (15 sec gas blank, 30 sec ablation) that excavated a pit ~25 µm deep. Ablated material was carried by a 1.2 L/min He gas stream to the nebulizer flow of the plasma. Dwell times were 5 ms for Si and Zr, 200 ms for ^{49}Ti and ^{207}Pb, 80 ms for ^{206}Pb, 40 ms for ^{202}Hg, ^{204}Pb, ^{208}Pb, ^{232}Th, and ^{238}U, and 10 ms for all other HFSE and REE. Background count rates for each analyte were obtained before each spot analysis and subtracted from the raw count rate for each analyte. Ablations pits that appear to have intersected glass or mineral inclusions were identified based on Ti and P. U-Pb dates from these analyses are considered valid if the U-Pb ratios appear to have been unaffected by the inclusions. Analyses that appear contaminated by common Pb were rejected based on mass 204 being above baseline. For concentration calculations, background-subtracted count rates for each analyte were internally normalized to ^{29}Si and calibrated with respect to NIST SRM-610 and -612 glasses as the primary standards. Temperature was calculated from the Ti-in-zircon thermometer (Watson et al., 2006). Because there are no constraints on the activity of TiO_2, an average value in crustal rocks of 0.8 was used. Errors on the mean temperatures are given at 1 sigma level. Errors on trace element concentrations are also given at 1 sigma level.

Data were collected in two experiments in February 2015. For U-Pb and $^{207}Pb/^{206}Pb$ dates, instrumental fractionation of the background-subtracted ratios was corrected, and dates were calibrated with respect to interspersed measurements of a zircon standard, Plešovice (Sláma et al., 2008), that was used to monitor time-dependent instrumental fractionation based on two analyses for every 10 analyses of unknown zircon. A polynomial fit to the standard analyses yields each sample-specific fractionation factor. Zircon standards Seiland (531 Ma, Kuiper et al., 2022) and Zirconia (327 Ma, unpublished data, Boise State University) were treated as unknowns and measured once for every 10 analyses of unknown zircon. These results are given in folder '2014-2019_BSU', Excel file 'GF2025-14_BSU_LA-ICPMS_results.xlsx', Table S3 (Appendix 1). Radiogenic isotope ratio and age error propagation includes uncertainty contributions from counting statistics and background subtraction.

Age interpretations are based on $^{206}Pb/^{238}U$ dates. Analyses with discordance, defined as the relative difference between the $^{207}Pb/^{235}U$ and $^{206}Pb/^{238}U$ dates, outside of uncertainty of 5% were removed from the data in folder '2014-2019_BSU', Excel file 'GF2025-14_BSU_LA-ICPMS_results.xlsx', Table S2 (Appendix 1). Errors are given at 2 sigma level.

2.3.2. CA-TIMS methods

U-Pb dates were obtained by the chemical abrasion isotope dilution thermal ionization mass spectrometry (CA-TIMS) method from analyses of single zircon grains. For seven samples, grains were selected based on CL images; for one sample, grains were selected based on LA-ICPMS data.

Single zircon grains were placed in a muffle furnace at 900°C for 60 hours in quartz beakers. The individual grains were then transferred to 3 ml Teflon PFA beakers and loaded into 300 µl Teflon PFA microcapsules. Fifteen microcapsules were placed in a large-capacity Parr vessel and the grains partially dissolved in 120 µl of 29 M HF for 12 hours at 180°C. The contents of the microcapsules were returned to 3 ml Teflon PFA beakers, HF removed, and the residual grains immersed in 3.5 M HNO_3, ultrasonically cleaned for an hour, and fluxed on a hotplate at 80°C for an hour. The HNO_3 was removed, and grains were rinsed twice in ultrapure H_2O before being reloaded into the 300 µl Teflon PFA microcapsules (rinsed and fluxed in 6 M HCl during sonication and washing of the grains) and spiked with the Boise State University mixed ^{233}U-^{235}U-^{205}Pb tracer solution. Zircon was dissolved in Parr vessels in 120 µl of 29 M HF with a trace of 3.5 M HNO_3 at 220°C for 48 hours, dried to fluorides, and re-dissolved in 6 M HCl at 180°C overnight. U and Pb were separated from the zircon matrix using an HCl-based anion-exchange chromatographic procedure (Krogh, 1973), eluted together and dried with 2 µl of 0.05 NH_3PO_4.

Pb and U were loaded on a single outgassed Re filament in 5 µl of a silica-gel/phosphoric acid mixture (Gerstenberger and Haase, 1997), and U and Pb isotopic measurements made on a GV Isoprobe-T multicollector thermal ionization mass spectrometer equipped with an ion-counting Daly detector. Pb isotopes were measured by peak-jumping all isotopes on the Daly detector for 100 to 160 cycles, and corrected for 0.16 ± 0.03%/a.m.u (1 sigma level error) mass fractionation. Transitory isobaric interferences due to high-molecular weight organics, particularly on ^{204}Pb and ^{207}Pb, disappeared within approximately 30 cycles, while ionization efficiency averaged 104 cps/pg of each Pb isotope. Linearity (to ≥1.4 x 10^6 cps) and the associated deadtime correction of the Daly detector were monitored by repeated analyses of NBS982 and have been constant since installation. Uranium was analyzed as UO_2^+ ions in static Faraday mode on 10^{12} ohm resistors for 200-300 cycles and corrected for isobaric interference of $^{233}U^{18}O^{16}O$ on $^{235}U^{16}O^{16}O$ with an $^{18}O/^{16}O$ of 0.00206. Ionization efficiency averaged 20 mV/ng of each U isotope. U mass fractionation was corrected using the known $^{233}U/^{235}U$ ratio of the Boise State University tracer solution.

U-Pb dates and uncertainties were calculated using the algorithms of Schmitz and Schoene (2007), $^{235}U/^{205}Pb$ of 77.93 and $^{233}U/^{235}U$ of 1.007066 for the Boise State University tracer solution, and U decay constants recommended by Jaffey et al. (1971). $^{206}Pb/^{238}U$ ratios and dates were corrected for initial ^{230}Th disequilibrium using a Th/U[magma] = 3.0 ± 0.3 using the algorithms of Crowley et al. (2007), resulting in an increase in the $^{206}Pb/^{238}U$ dates of ~0.09 Ma. All common Pb in analyses was attributed to laboratory blank and subtracted based on the measured laboratory Pb isotopic composition and associated uncertainty. U blanks are difficult to precisely measure, but are estimated at 0.07 pg.

Weighted mean $^{206}Pb/^{238}U$ dates are calculated from equivalent dates (probability of fit >0.05) using Isoplot 3.0 (Ludwig, 2003) with error at the 95% confidence interval. Error is computed as the internal standard deviation multiplied by the Student's t-distribution multiplier for a two-tailed 95% critical interval and n-1 degrees of freedom when the reduced chi-squared statistic, mean squared weighted deviation (MSWD) (Wendt and Carl, 1991), takes a value less than its expectation value plus its standard deviation at the same confidence interval, which is when MSWD is <1+2*sqrt[2/(n-1)]. This error is expanded via multiplication by the sqrt(MSWD) when the MSWD is ≥1+2*sqrt[2/(n-1)] to accommodate unknown sources of over dispersion. Errors on the weighted mean dates are given as ± x / y / z, where x is the internal error based on analytical uncertainties only, including counting statistics, subtraction of tracer solution, and blank and initial common Pb subtraction, y includes the tracer calibration uncertainty propagated in quadrature, and z includes the ^{238}U decay constant uncertainty (Jaffey et al., 1971) propagated in quadrature. Internal errors should be considered when comparing Boise State University dates with $^{206}Pb/^{238}U$ dates from other laboratories that used the same tracer solution or a tracer solution that was cross-calibrated using EARTHTIME gravimetric standards. Errors including the uncertainty in the tracer calibration should be considered when comparing Boise State University dates with those derived from other geochronological methods using the U-Pb decay scheme (e.g., LA-ICPMS). Errors including uncertainties in the tracer calibration and ^{238}U decay constant should be considered when comparing Boise State University dates with those derived from other decay schemes (e.g., $^{40}Ar/^{39}Ar$, $^{187}Re-^{187}Os$). Results are given in folder '2014-2019_BSU', Excel file 'GF2025-14_BSU_CA-TIMS_results.xlsx' (Appendix 1). Errors on dates from individual analyses are given at 2 sigma level.

2.4. 2023 samples

Three samples collected in 2023 underwent mineral separation at Zirchron LLC and were analyzed at PCIGR.

2.4.1. LA-ICPMS methods

Zircons were mounted in epoxy, along with reference materials. Grain mounts were wet ground with carbide abrasive paper and polished with diamond paste. Cathodoluminescence (CL) imaging was carried out on a Philips XL-30 scanning electron microscope (SEM) equipped with a Bruker Quanta 200 energy-dispersion X-ray microanalysis system at the Electron Microbeam/Xray Diffraction Facility (EMXDF) at the University of British Columbia. An operating voltage of 15 kV was used, with a spot diameter of 6 µm and peak count time of 17-27 seconds. After removal of the carbon coat the grain mount surface was washed with mild soap and rinsed with high purity water. Before analysis the grain mount surface was cleaned with 3 N HNO_3 acid and again rinsed with high purity water to remove any surficial Pb contamination that could interfere with the early portions of the spot analyses.

Analyses were conducted using a Resonetics RESOlution M-50-LR, which contains a Class I laser device equipped with a UV excimer laser source (Coherent COMPex Pro 110, 193 nm, pulse width of 4 ns) and a two-volume cell designed and developed by Laurin Technic Pty. Ltd. (Australia). This sample chamber allowed investigating several grain mounts in one analytical session. The laser path was fluxed by N_2 to ensure better stability. Ablation was carried out in a cell with a volume of approximately 20 cm^3 and a He gas stream that ensured better signal stability and lower U-Pb fractionation (Eggins et al., 1998). The laser cell was connected via a Teflon squid to an Agilent 7700x quadrupole ICP-MS housed at PCIGR. A pre-ablation shot was used to ensure that the spot area on grain surface was contamination-free. Samples and reference materials were analyzed for 36 isotopes: ^{7}Li, ^{29}Si, ^{31}P, ^{43}Ca, ^{45}Sc, ^{49}Ti, ^{89}Y, ^{91}Zr, ^{93}Nb, ^{139}La, ^{140}Ce, ^{141}Pr, ^{146}Nd, ^{147}Sm, ^{153}Eu, ^{157}Gd, ^{159}Tb, ^{163}Dy, ^{165}Ho, ^{166}Er, ^{169}Tm, ^{172}Lu, ^{177}Hf, ^{181}Ta, ^{202}Hg, Pb (^{204}Pb, ^{206}Pb, ^{207}Pb, ^{208}Pb), ^{232}Th, and U (^{235}U, ^{238}U) with a dwell time of 0.02 seconds for each isotope. Pb/U and Pb/Pb ratios were determined on the same spots along with trace element concentration determinations. These isotopes were selected based on their relatively high natural abundances and absence of interferences. The settings for the laser were: spot size of 34 µm with a total ablation time of 30 seconds, frequency of 5 Hz, fluence of 5 J/cm^2, power of 7.8 mJ after attenuation, pit depths of approximately 15 µm, He flow rate of 800 mL/min, N_2 flow rate of 2 mL/min, and a carrier gas (Ar) flow rate of 0.57 L/min.

Reference materials were analyzed throughout the sequence to allow for drift correction and to characterize downhole fractionation for Pb/U and Pb/Pb isotopic ratios. For trace elements, NIST 612 glass was used for both drift correction and trace element calibration, with sample spacing between every five to eight unknowns, and ^{90}Zr was used as the internal standard assuming stoichiometric values for zircon. NIST

610 glass was analyzed after each NIST 612 analysis and used as a monitor reference material for trace elements. For U-Pb analyses, natural zircon reference materials were used, including Plešovice (Sláma et al., 2008; 337.13 ±0.33 Ma) or 91500 (Wiedenbeck et al., 1995; 2004; 1062.4 ±0.4 Ma, $^{206}Pb/^{238}U$ date) as the internal reference material, and both Temora2 (Black et al., 2004; 416.78 ±0.33 Ma) and Plešovice and/or 91500 as monitoring reference materials; the zircon reference materials were placed between the unknowns in a similar fashion as the NIST glasses. Raw data were reduced using the Iolite 3.4 extension (Paton et al., 2011) for Igor Pro™ yielding concentration values, Pb/U and Pb/Pb dates, and their respective propagated uncertainties. Weighted mean $^{206}Pb/^{238}U$ dates were calculated using IsoplotR (Vermeesch, 2018). Results are given in folder '2023_PCIGR', Excel file 'GF2025-14_PCIGR_LA-ICPMS_results.xlsx' (Appendix 1).

3. Sample descriptions and analytical results

Samples and analytical results are described below from oldest to youngest. We report nine samples from the Stikine plutonic suite (Late Triassic), one sample from the Galore plutonic suite (Late Triassic), three samples from the Cone Mountain plutonic suite (late Early Jurassic), five samples from subvolcanic feeders to the upper Hazelton Group and/or the Three Sisters plutonic suite (late Early Jurassic to Middle Jurassic), and one sample from an unassigned Late Cretaceous plutonic suite.

3.1. Stikine plutonic suite (Late Triassic)

3.1.1. Hickman pluton

3.1.1.1. Sample LB-14-069

We sampled a plagioclase-megacrystic hornblende diorite (Fig. 2a) from an approximately 30 km^2 intrusive body of the same texture and composition on the western side of the Hickman pluton (Fig. 1). This intrusion crosscuts ultramafic rocks of the Middle Scud ultramafic body and is crosscut by granodiorite dikes that are similar in composition to the main phase of the Hickman pluton (e.g., sample LB-14-132 below).

Six zircon grains from sample LB-14-069 analyzed by CA-TIMS yielded a weighted mean $^{206}Pb/^{238}U$ date of 222.31 ± 0.07 / 0.10 / 0.26 Ma (MSWD = 1.6, probability = 0.16; Fig. 3a), which is interpreted as the igneous crystallization age.

The new age corroborates crosscutting relationships and demonstrates that the plagioclase-megacrystic diorite to quartz diorite unit (Brown et al., 1996; Campbell and van Straaten, 2025) is older than the main phase of the Hickman pluton (see below).

3.1.1.2. Sample LB-14-227

We sampled a fine-grained syenite to quartz monzonite from the central part of the Hickman pluton (Fig. 1). Based on observations elsewhere in the Hickman pluton, this intrusion was presumed to be younger than the granodiorite at station LB-14-132. However, no crosscutting relationships were observed at this sample location.

Thirty-five zircon grains from sample LB-14-227 analyzed by LA-ICPMS yield a weighted mean $^{206}Pb/^{238}U$ date of 221 ± 4 Ma (MSWD = 0.8). The zircon grains have chemistry that is typical of zircon from arc magmas (Boise State University,

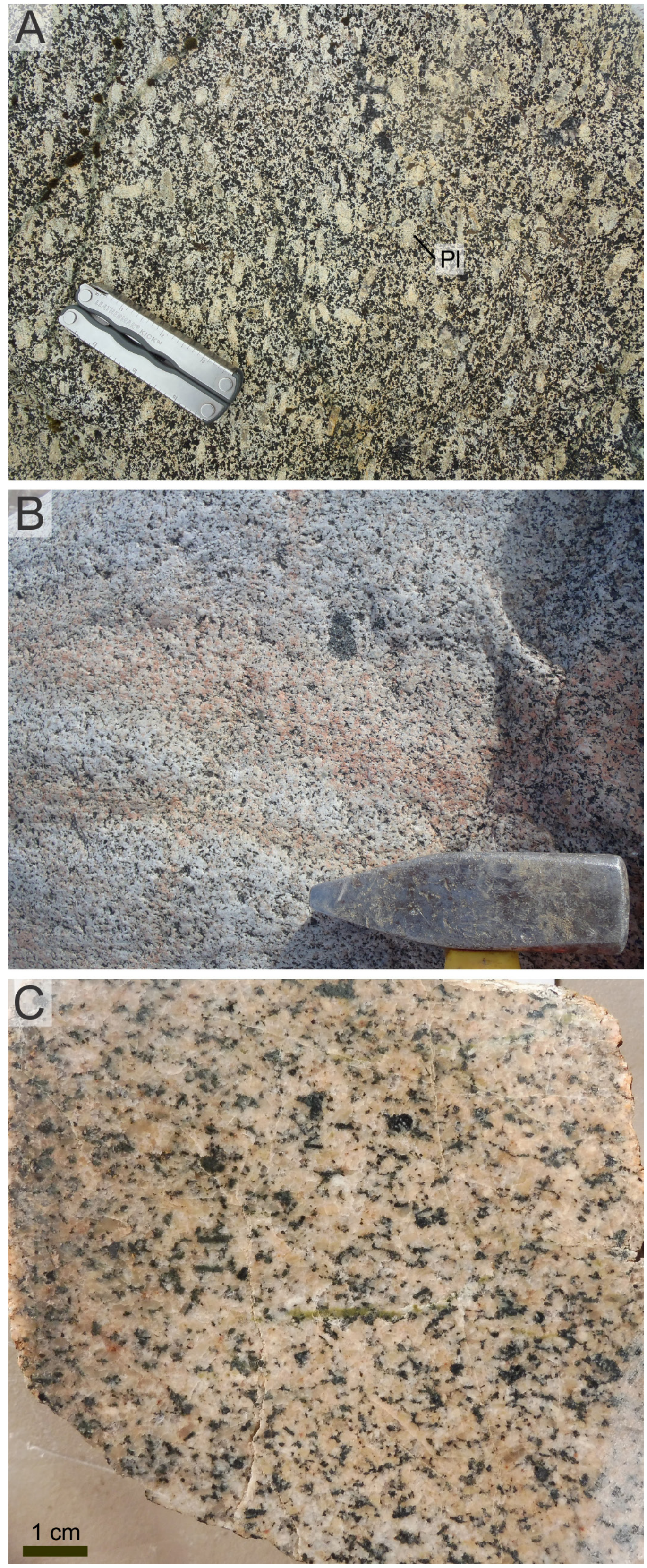

Fig. 2. Stikine plutonic suite, Hickman pluton. **a)** Plagioclase (Pl)-megacrystic hornblende diorite sample LB-14-069. **b)** Main phase of the Hickman pluton, representative of sample LB-14-132. **c)** Granodiorite sample SCK-2013-MLT-011HA.

unpublished data) and the Ti-in-zircon result is 785 ± 33°C. Five zircon grains analyzed by CA-TIMS yield a weighted mean $^{206}Pb/^{238}U$ date of 221.67 ± 0.09 / 0.11 / 0.27 Ma (MSWD = 1.7, probability = 0.16; Fig. 3b), which is interpreted as the igneous crystallization age.

The sample lithology suggests a possible correlation with the quartz monzonite unit (LTrSdqm) of Campbell and van Straaten (2025). The new age overlaps with the age obtained for granodiorite from the Hickman pluton (see sample LB-14-132 below), suggesting compositionally variable coeval phases during this stage of pluton formation.

3.1.1.3. Sample LB-14-132

We sampled an equigranular granodiorite from the west-central portion of the Hickman pluton (Fig. 1). The sample contains 30% hornblende and biotite, 20% quartz, 10% K-feldspar, and 40% plagioclase. The composition and texture of this sample is representative of the main phase of the Hickman pluton (Fig. 2b).

Six zircon grains from sample LB-14-132 analyzed by CA-TIMS yield a weighted mean $^{206}Pb/^{238}U$ date of 221.52 ± 0.08 / 0.10 / 0.26 Ma (MSWD = 1.1, probability = 0.35; Fig. 3c), which is interpreted as the igneous crystallization age.

The new age constrains the emplacement of the main phase of the Hickman pluton (LTrSgd, granodiorite to quartz monzodiorite unit of Campbell and van Straaten, 2025).

3.1.1.4. Sample SCK-2013-MLT-011HA

We sampled a medium-grained equigranular biotite-hornblende granodiorite from the northeastern portion of the

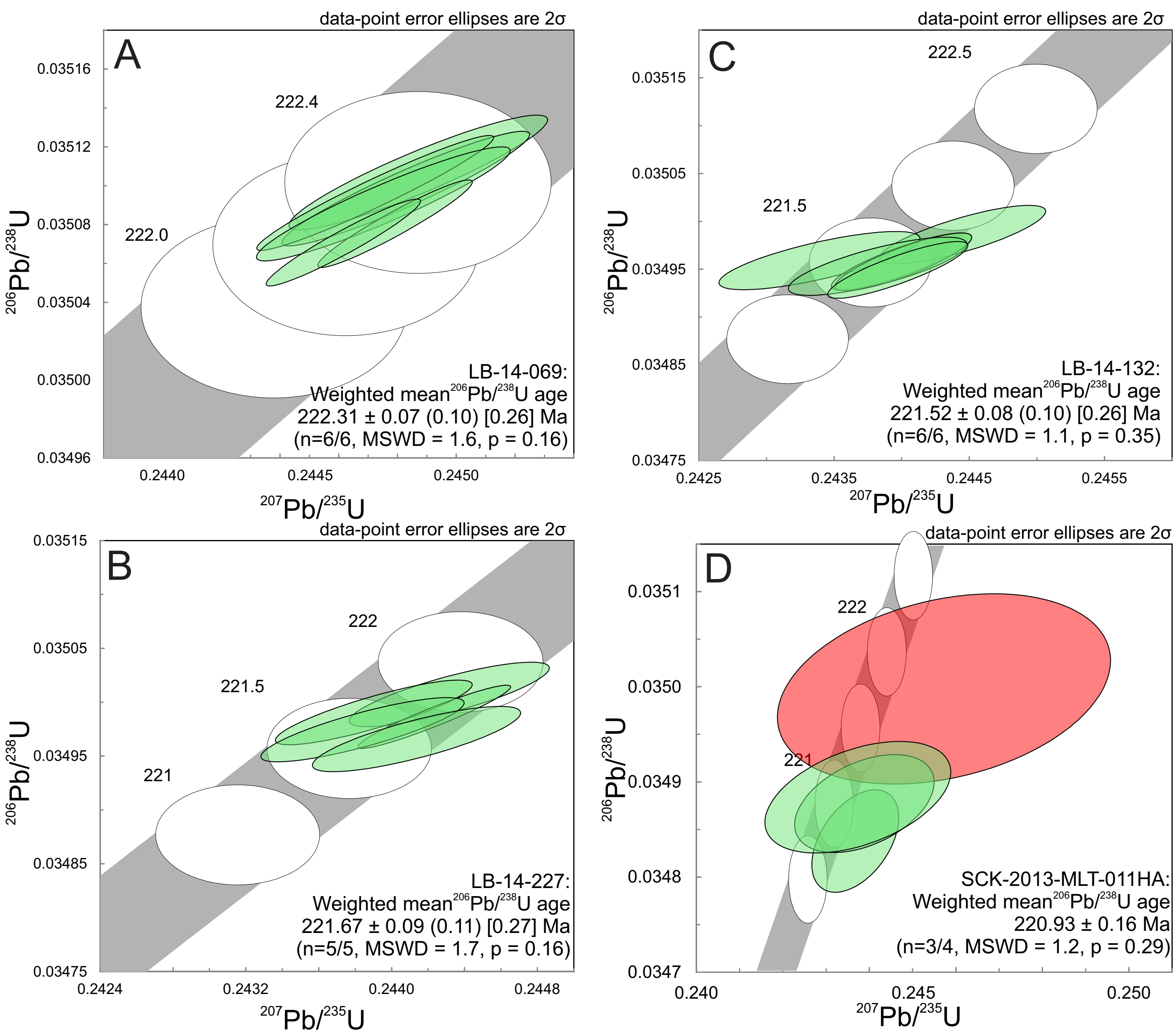

Fig. 3. Stikine plutonic suite, Hickman pluton. U-Pb zircon concordia diagrams with **a)** CA-TIMS results from sample LB-14-069, **b)** CA-TIMS results from sample LB-14-227, **c)** CA-TIMS results from sample LB-14-132, and **d)** CA-TIMS results from sample SCK-2013-MLT-011HA.

Hickman pluton (Fig. 1). The sample contains 15% hornblende, 5% biotite, 60% feldspar, 20% quartz, and trace titanite and magnetite (Fig. 2c). The sample shows no significant hydrothermal alteration or mineralization. The granodiorite is cut by numerous mafic dikes (<1 m wide).

Four zircon grains were analyzed by CA-TIMS. The three youngest zircon grains yield a weighted mean $^{206}Pb/^{238}U$ date of 220.93 ± 0.16 Ma (MSWD = 1.2, probability = 0.29; Fig. 3d), which is interpreted as the igneous crystallization age. The oldest grain yields a 221.76 ± 0.51 Ma date, interpreted as an antecryst.

The two new ages for the main phase of the Hickman pluton (LTrSgd of Campbell and van Straaten, 2025) suggest that it crystallized during an interval of at least 0.59 ± 0.24 m.y.

3.1.2. Equigranular intrusions at the Schaft Creek deposit

3.1.2.1. Sample GJ-14-002

We sampled an equigranular granodiorite north of the LaCasse showing (MINFILE 104G 190). This sample is texturally and compositionally similar to the main phase of the Hickman pluton. At the sample site, granodiorite is crosscut by syenite dikes similar to those sampled at station GJ-14-001 (see Section 3.4.4.).

Forty zircon grains from sample GJ-14-002 analyzed by LA-ICPMS yield a weighted mean $^{206}Pb/^{238}U$ date of 216 ± 4 Ma (MSWD = 1.5). Zircon grains have a chemistry that is typical of zircon from arc magmas (Boise State University, unpublished data) and the Ti-in-zircon result is 744 ± 40°C. Six zircon grains analyzed by CA-TIMS yield a weighted mean $^{206}Pb/^{238}U$ date of 220.92 ± 0.08 / 0.11 / 0.26 Ma (MSWD = 2.0, probability = 0.08; Fig. 5a), which is interpreted as the igneous crystallization age.

3.1.2.2. Sample 08CF326-76m

We sampled a quartz monzodiorite (logging code QMZ; Jutras and Bailey, 2016; Erbalaban, 2023) from the West Breccia zone of the Schaft Creek deposit. The sample is medium-grained, equigranular to weakly porphyritic, and contains 5% quartz phenocrysts and 15% hornblende. Hornblende is altered to pyrite and chlorite, and the groundmass is weakly chlorite and albite altered.

Fig. 4. Stikine plutonic suite, equigranular intrusions at the Schaft Creek deposit. Equigranular granodiorite from drill hole 08CF364 at 28.3-28.8 m (same lithology as sample 08CF364-31.7m).

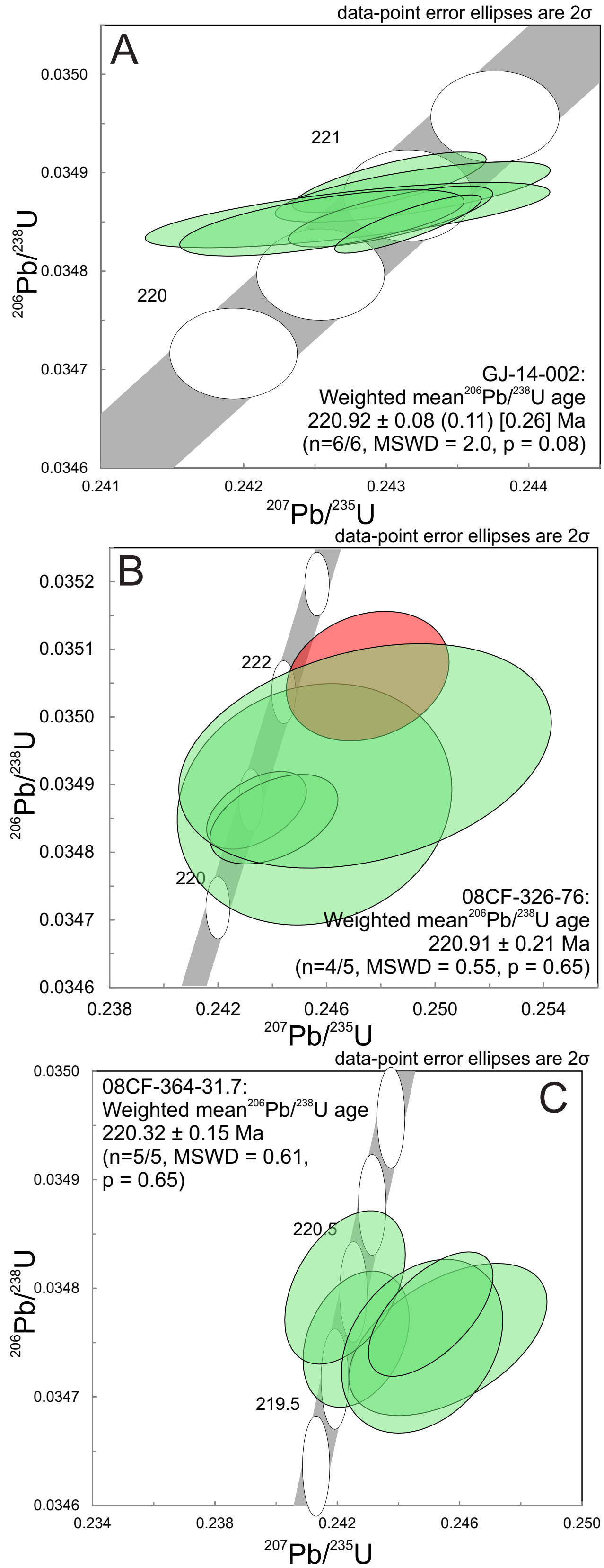

Fig. 5. Stikine plutonic suite, equigranular intrusions at the Schaft Creek deposit. U-Pb zircon concordia diagrams with **a)** CA-TIMS results from sample GJ-14-002, **b)** CA-TIMS results from sample 08CF-326-76, and **c)** CA-TIMS results from sample 08CF-384-31.7.

Five zircon grains were analyzed by CA-TIMS. The four youngest zircon grains yield a weighted mean $^{206}Pb/^{238}U$ date of 220.91 ± 0.21 Ma (MSWD = 0.55, probability = 0.65; Fig. 5b), which is interpreted as the igneous crystallization age. The oldest grain returned a 221.41 ± 0.85 Ma date, interpreted as an antecryst.

3.1.2.3. Sample 08CF364-31.7m

We sampled a medium-grained equigranular granodiorite (logging code GRD; Jutras and Bailey, 2016; Erbalaban, 2023) from the Paramount zone of the Schaft Creek deposit. The sample contains 20% quartz, 65% feldspar, and 15% tabular to irregular chlorite-altered mafic minerals (possibly hornblende; Fig. 4).

Five zircon grains analyzed by CA-TIMS yield a weighted mean $^{206}Pb/^{238}U$ date of 220.32 ± 0.15 Ma (MSWD = 0.61, probability = 0.65; Fig. 5c), which is interpreted as the igneous crystallization age.

We report three new ages for equigranular intrusions at the Schaft Creek deposit. The two oldest ages (ca. 220.9 Ma) overlap each other and the youngest age from the main phase of the Hickman pluton. The youngest age (ca. 220.3 Ma) does not overlap with the older two ages but overlaps with a CA-TIMS U-Pb zircon age obtained from granodiorite of the Nightout pluton (220.36 ± 0.13 Ma; van Straaten, 2024).

3.1.3. Porphyritic intrusions at the Schaft Creek deposit

3.1.3.1. Sample P69CH02-32m

We sampled a porphyritic quartz monzodiorite dike (logging code sPOR; Jutras and Bailey, 2016; Erbalaban, 2023), from the Paramount zone of the Schaft Creek deposit. The sample is a medium grey, moderately crowded hornblende-plagioclase porphyry with 20% equant subhedral-euhedral plagioclase (0.5-2 mm), 10% hornblende, and minor miarolitic cavities set in a fine-grained groundmass (Fig. 6a). The porphyritic intrusion is cut by magnetite-K-feldspar veins, and cuts equigranular granodiorite (logging code GRD) intersected further down the hole (below 36.9 m). A more crowded porphyritic intrusion intersected up hole (14.0-29.3 m) contains andesite and equigranular granodiorite xenoliths.

Five zircon grains were analyzed by CA-TIMS. The four youngest grains yielded a weighted mean $^{206}Pb/^{238}U$ date of 219.43 ± 0.18 Ma (MSWD = 0.96, probability = 0.41; Fig.

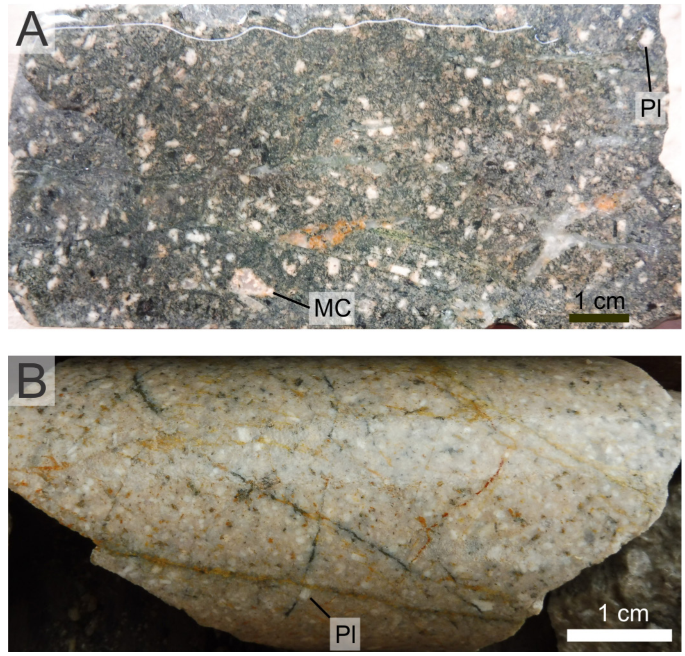

Fig. 6. Stikine plutonic suite, porphyritic intrusions at the Schaft Creek deposit. **a)** Moderately crowded plagioclase (Pl) porphyry with minor miarolitic cavities (MC) from drill hole P69CH02 at 30.5 m (same lithology as sample P69CH02-32m). **b)** Crowded plagioclase porphyry from drill hole H69CH046 at 255.8 m (same lithology as sample H69CH046-249.8m).

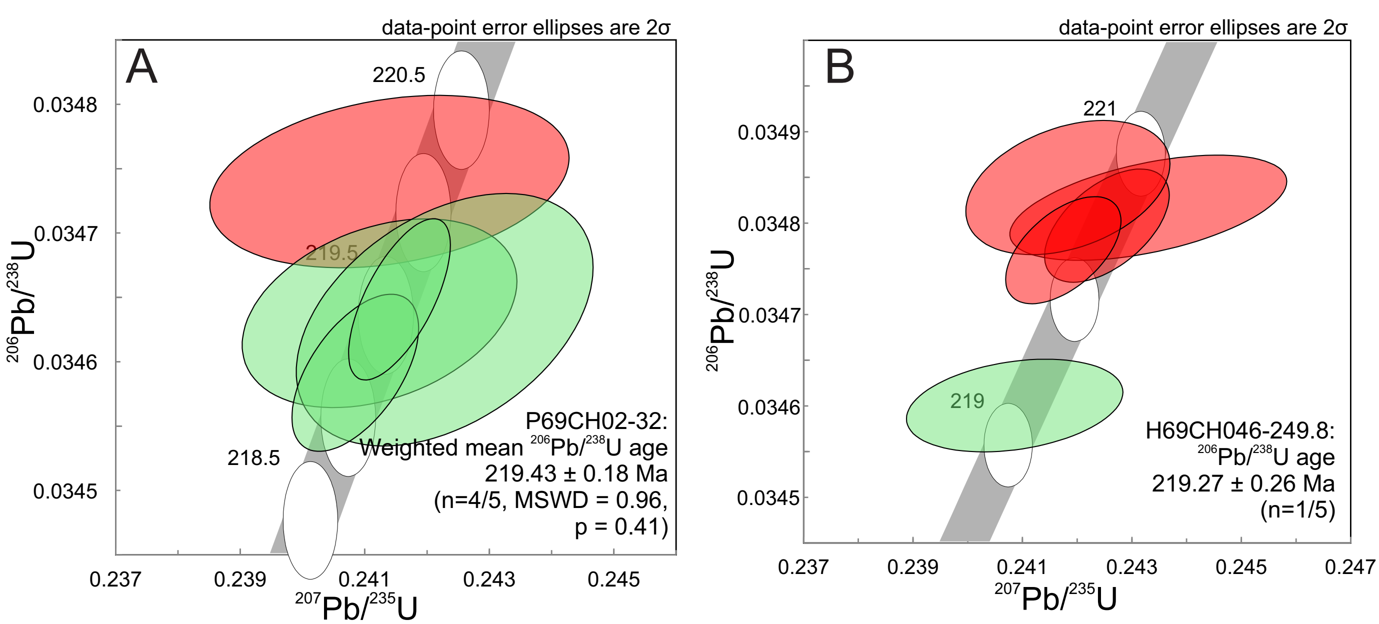

Fig. 7. Stikine plutonic suite, porphyritic intrusions at the Schaft Creek deposit. U-Pb zircon concordia diagrams with **a)** CA-TIMS results from sample P69CH02-32, and **b)** CA-TIMS results from sample H69CH046-249.8.

7a), which is interpreted as the igneous crystallization age. The oldest grain yielded a 220.15 ± 0.34 Ma date and is interpreted as an antecryst.

3.1.3.2. Sample H69CH046-249.8m

We sampled a porphyritic quartz monzodiorite dike (logging code sPOR; Jutras and Bailey, 2016; Erbalaban, 2023) from the central Liard zone of the Schaft Creek deposit. The sample is a crowded porphyry with 50% weakly albitized and chloritized plagioclase, 8% chlorite-sericite-altered mafic minerals (biotite and possible hornblende), and 2% quartz (Fig. 6b). The intrusion contains disseminated bornite and chalcopyrite, and is cut by hairline bornite veinlets, quartz-chalcopyrite veinlets, and quartz-molybdenite veins. The intrusion becomes moderately crowded (25% plagioclase, 10% mafic minerals, and 2% quartz) towards a lower contact (at 279.8 m) with medium-grained equigranular quartz monzodiorite. Farther down the drill hole, the equigranular quartz monzodiorite is cut by two narrow plagioclase porphyry dikes containing 20-45% plagioclase, 20% mafic minerals, trace quartz, and minor disseminated and veinlet-hosted chalcopyrite.

Five zircon grains were analyzed by CA-TIMS. The youngest zircon grain yielded a $^{206}Pb/^{238}U$ date of 219.27 ± 0.26 Ma (Fig. 7b), which is interpreted as the igneous crystallization age. Four older concordant grains yield a weighted mean $^{206}Pb/^{238}U$ date of 220.54 ± 0.16 Ma (MSWD = 1.2, probability = 0.30) and are interpreted as antecrysts.

Two new ages for porphyritic intrusions suggest mineralization at Schaft Creek occurred ca. 219.4-219.3 Ma or younger. The spatial coincidence of these porphyritic intrusions and mineralization at the Schaft Creek deposit suggests these may represent syn-mineral intrusions. A total of five inherited grains from the two syn-mineral intrusion samples are ca. 220.5-220.2 Ma and overlap with ages for equigranular intrusions at the Schaft Creek deposit (see Section 3.1.2.).

3.2. Galore plutonic suite (Late Triassic)

3.2.1. Sample ABA05-46-369

We sampled an equigranular syenite for U-Pb geochronology from a composite intrusive body east of Mount Scotsimpson (Fig. 1). Petrographic observations show a medium-grained equigranular syenite containing 70% partially altered feldspar (at least two third K-feldspar, no more than one third plagioclase), 25% mafic minerals (clinopyroxenite, lesser biotite, and rare hornblende), 2% apatite, 2% opaque minerals, 1% quartz, and trace titanite.

Four zircon fractions were analyzed by ID-TIMS and yielded a concordia age of 204.45 ± 0.69 Ma (MSWD = 1.18, probability = 0.28), and a weighted mean $^{206}Pb/^{238}U$ date of 204.5 ± 1.0 Ma (MSWD = 4.0, probability = 0.007; Fig. 8). The weighted mean $^{206}Pb/^{238}U$ date, with more conservative errors, is interpreted as the crystallization age.

The 5 km^2 northeast-trending intrusive body consists primarily of porphyritic monzodiorite to monzonite, trachytic quartz syenite porphyry, and lesser medium-grained diorite. The intrusive rocks contain medium grained (2-3 mm), equigranular interlocking crystals, including 30% K-feldspar, 25% hornblende, 20% plagioclase, 10% epidote, <5% biotite, and <5% quartz; the remaining 15-20% of the rock is made up

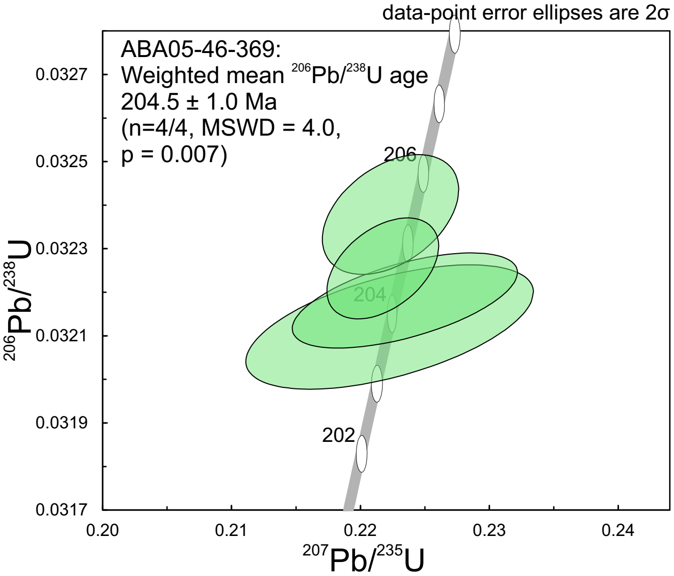

Fig. 8. Galore plutonic suite. U-Pb zircon concordia diagram with ID-TIMS results from sample ABA05-46-369.

of tabular white K-feldspar phenocrysts (5-15 mm). The stock is heterogeneous and intermixed with or veined by more potassic phases. The rocks are overprinted by a moderate propylitic alteration assemblage of epidote, chlorite, pyrite, and quartz. The intrusive body was previously assigned to the Texas Creek plutonic suite (Early Jurassic; Logan and Koyanagi, 1994). Based on the Late Triassic U-Pb zircon age and subsequent detailed mapping by Galore Creek Mining Corporation, this body has been re-assigned to a monzodioritic to syenitic unit of the Galore plutonic suite (Logan et al. map in Prince, 2020). The new U-Pb age appears to suggest that Galore plutonic suite intrusions range in age from at least 210 to 204 Ma (Mortensen et al., 1995; Coulson et al., 1999; Logan and Mihalynuk, 2014; Enduro Metals Corp., 2021).

3.3. Cone Mountain plutonic suite (late Early Jurassic)

3.3.1. Sample RK23-034

We sampled a coarse-grained, equigranular, biotite quartz monzonite (Fig. 9a) from near the southeastern margin of the Pereleshin pluton (Fig. 1).

Sixty zircon grains from sample RK23-034 were analyzed by LA-ICPMS and yielded a weighted mean $^{206}Pb/^{238}U$ date of 185 ± 1 Ma (MSWD = 0.86, probability = 0.78; Fig. 10a), which is interpreted as the igneous crystallization age.

The ~180 km^2 Pereleshin pluton was previously mapped by Logan and Koyanagi (1994) and Brown et al. (1996), and they described it as a medium- to coarse-grained, K-feldspar megacrystic to equigranular, hornblende to hornblende-biotite quartz monzonite to granite. Based on compositional criteria they assigned it to the Texas Creek plutonic suite (Early Jurassic). Along a traverse across the southeastern portion of the pluton we observed a coarse-grained hornblende-biotite quartz monzonite to granite unit that closely resembles the description by Logan and Koyanagi (1994) and Brown et al. (1996). Observations in the southwestern part of the pluton (approximately 4 km west of sample RK23-034) showed predominantly medium-grained

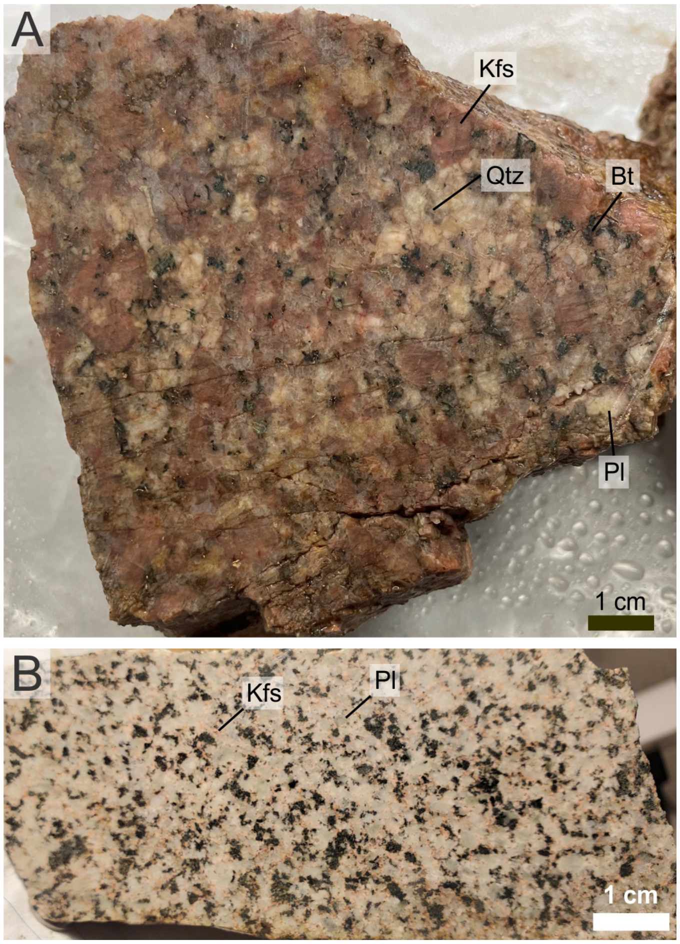

Fig. 9. Cone Mountain plutonic suite. **a)** Pereleshin pluton, coarse-grained quartz monzonite sample RK23-034. **b)** Scud River stock, quartz monzodiorite to quartz monzonite from station 24RCA-199a (same location as sample LB-14-218). Pl: plagioclase, Kfs: K-feldspar, Qtz: quartz, Bt: biotite.

hornblende-biotite quartz monzonite with approximately 30% plagioclase, 30% K-feldspar, 10-15% quartz, and 10-20% chloritized mafic minerals. The new age suggests that the Pereleshin pluton is part of the Cone Mountain plutonic suite.

3.3.2. Sample LB-14-218

We sampled a porphyritic quartz monzodiorite to quartz monzonite containing 20% mafic minerals (Fig. 9b) from the southeastern portion of the Scud River stock (Fig. 1).

Forty-six zircon grains from sample LB-14-218 analyzed by LA-ICPMS yield a weighted mean of 181 ± 4 Ma (MSWD = 0.7). Zircon grains have a chemistry that is typical of zircon from arc magmas (Boise State University, unpublished data) and the Ti-in-zircon result is 717 ± 17°C. Six zircon grains analyzed by CA-TIMS yielded a weighted mean date of 184.96 ± 0.07 / 0.09 / 0.22 Ma (MSWD = 1.0, probability = 0.41, Fig. 10b), which is interpreted as the igneous crystallization age.

The ~10 km^2 Scud River stock was previously mapped as a medium-grained, equigranular biotite monzonite to hornblende-biotite quartz monzonite, and assigned to the Texas Creek plutonic suite (Logan and Koyanagi, 1994). The late Early Jurassic U-Pb zircon age and subsequent detailed mapping by Galore Creek Mining Corporation assigned the

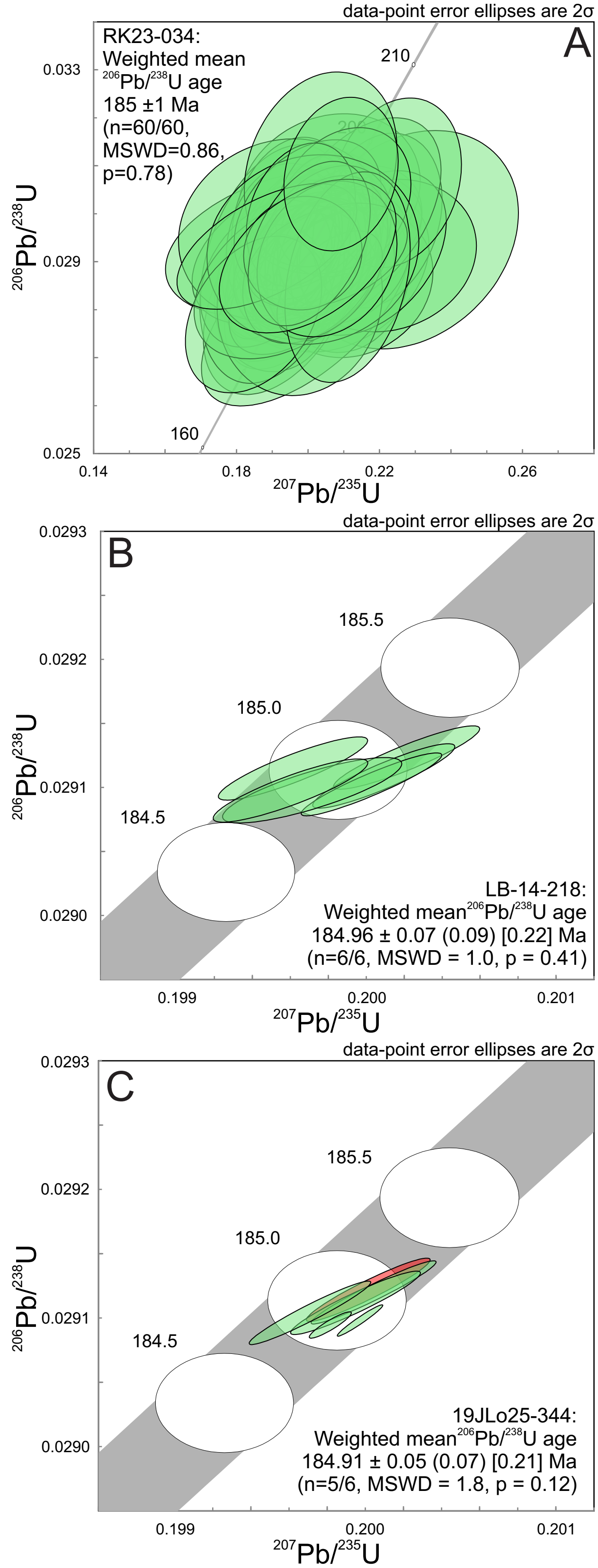

Fig. 10. Cone Mountain plutonic suite. U-Pb concordia diagrams with **a)** LA-ICPMS results from sample RK23-034, **b)** CA-TIMS results from sample LB-14-218, and **c)** CA-TIMS results from sample 19JLo25-344.

Scud River stock to a hornblende biotite granodiorite unit of the Cone Mountain plutonic suite (Logan et al. map in Prince, 2020).

3.3.3. Sample 19JLo25-344

We sampled a small, unnamed equigranular hornblende quartz monzonite body approximately 5 km north of the Copper canyon deposit (Fig. 1). The quartz monzonite intrudes massive plagioclase-pyroxene porphyry basalt flows and breccias of the Stuhini Group (Upper Triassic) and is truncated along its eastern margin by the Copper canyon thrust (part of the South Scud river fault zone). The eastern margin of the pluton is Fe-carbonate altered, contains pendants of harmonically folded volcanic sandstone, and discrete north-striking brittle shear zones parallel to the Copper canyon thrust fault. The sample site exposes pink-white weathering, massive, medium-grained, equigranular hornblende quartz monzonite, containing 30% tabular plagioclase (2-3 mm), 45% subhedral to interstitial orthoclase (3 mm), 15-20% hornblende (4-5 mm), 5-10% subhedral quartz, and minor disseminated magnetite.

Six zircon grains analyzed by CA-TIMS yielded a weighted mean of 184.91 ± 0.05 / 0.07 / 0.21 Ma (MSWD = 1.8, probability = 0.12; Fig. 10c), which is interpreted as the igneous crystallization age. One slightly older date of 185.05 ± 0.13 Ma is interpreted as antecrystic.

The ~1.8 km^2 plutonic body was initially assigned to the Stikine plutonic suite (Late Triassic; Logan and Koyanagi, 1994). However, based on the late Early Jurassic U-Pb zircon age, and subsequent detailed mapping by Galore Creek Mining Corporation it has been re-assigned to a hornblende biotite granodiorite unit of the Cone Mountain plutonic suite (Logan et al. map in Prince, 2020). Our three Cone Mountain plutonic suite samples range in composition from quartz monzonite to quartz monzodiorite and returned ca. 185 Ma crystallization ages, all within error of a 184.7 ± 0.6 Ma ID-TIMS U-Pb zircon age for a biotite-hornblende granodiorite sample from the Cone Mountain pluton (Brown et al., 1992; 1996). Our geochronology results significantly expand the known extent of this plutonic suite to a belt approximately 60 km long; the overlapping ages suggest that plutonism was short-lived.

The Cone Mountain plutonic suite intrusions are west of the Copper canyon thrust fault (part of the South Scud river fault zone). Observations at the plutonic body 5 km north of Copper canyon suggest folding of (likely Triassic) sedimentary strata pre-dates emplacement of the pluton, and latest movement on the Copper canyon thrust fault post-dates emplacement of the pluton. An unpublished report by P. Read (see Logan and Koyanagi, 1994) suggested the Copper canyon thrust fault is plugged by the Scud River stock. However, subsequent mapping (Logan and Koyanagi, 1994; Logan et al. in Prince, 2000) interpreted the Copper canyon thrust fault to merge with a subvertical northwest-trending fault that clearly cuts the pluton. A northwestward continuation of this fault system (Cone Mountain thrust fault) postdates emplacement of the Cone Mountain pluton (ca. 185 Ma; Brown et al., 1996).

3.4. Upper Hazelton Group and/or Three Sisters plutonic suite (late Early Jurassic to Middle Jurassic)

3.4.1. Sample RK23-037

We sampled a porphyritic quartz monzonite to granodiorite 2 km south-southeast of the Jay showing (MINFILE 104G 046; Fig. 1). The sample site exposes pink weathering, pale greenish-grey fresh, medium- to coarse-grained, biotite-quartz-feldspar porphyritic, biotite quartz monzonite to granodiorite containing 20% subrounded quartz, 30% plagioclase, 10% K-feldspar, and 5% biotite phenocrysts in a fine-grained groundmass with 0.1-0.5% molybdenite, 0.2% rusty disseminated pyrite, and possible trace galena (Fig. 11a).

Sixty zircon grains were analyzed by LA-ICPMS. Excluding two outliers, 58 grains yield a weighted mean $^{206}Pb/^{238}U$ date of 180.7 ± 1.2 Ma (MSWD = 0.85, probability = 0.79; Fig. 12a), which is interpreted as the igneous crystallization age.

The sample was taken from within a circular 0.6 by 0.6 km light-weathering intrusive body emplaced within darker-weathering mafic volcanic rocks of the Stuhini Group (Fig. 11b). Previously this body was mapped as being smaller and was assigned to an augite monzonite unit of the Stikine plutonic suite (unit lTrm of Logan and Koyanagi, 1994). The new age is significantly younger, with potential relationship to felsic magmatism feeding upper Hazelton Group volcanic rocks (e.g., Horn Mountain Formation, ca. 185-175 Ma; Brown et al., 1996; van Straaten, 2024).

3.4.2. Sample SCK14-SH836

We sampled a flow-banded felsic dike (Fig. 11c) at the LaCasse showing (MINFILE 104G 190). The dike crosscuts a phase of the mineralized breccia, which in turn cuts the Hickman pluton.

Forty-three zircon grains from sample SCK14-SH836 were analyzed by LA-ICPMS. The oldest 40 grains yielded a weighted mean date of 221 ± 4 Ma (MSWD = 1.2). These zircon grains have a chemistry that is typical of zircon from arc magmas (Boise State University, unpublished data) and the Ti-in-zircon result is 745 ± 42°C. CA-TIMS analysis of six grains from the oldest zircon population yielded dates of 221.32 ± 0.15 to 220.51 ± 0.15 Ma (Fig. 12b) and are interpreted as xenocrysts. The youngest three grains yielded a weighted mean LA-ICPMS date of 182 ± 7 Ma (MSWD = 1.0). These grains have a chemistry that is typical of zircon from small volume felsic arc magmas (Boise State University, unpublished data) with the ~179 Ma zircon having high total REE (1680 ± 461 ppm) and U (321 ± 65 ppm) concentrations relative to the older ~221 Ma xenocrystic zircon (total REE 498 ± 208 ppm, U 115 ± 46 ppm). The Ti-in-zircon result is 729 ± 9°C. CA-TIMS analysis of these three grains yielded a weighted mean date of 178.85 ± 0.20 / 0.21 / 0.28 Ma (MSWD = 0.3, probability = 0.74; Fig. 12c), which is interpreted as the igneous crystallization age.

The lithology and age of this sample suggests that the felsic dikes acted as feeders to volcanic rocks in the upper Hazelton Group (Horn Mountain Formation, ca. 185-175 Ma; Brown et al., 1996; van Straaten, 2024).

3.4.3. Sample 2010CF401-140m

We sampled a porphyry dike (logging code pPOR; Jutras and Bailey, 2016; Erbalaban, 2023) from the Paramount zone of the Schaft Creek deposit. The dike is chlorite-epidote-calcite altered and contains 25% plagioclase phenocrysts (up to 2 mm), 5-10% pyroxene (0.1-1 mm), and trace pyrite in an aphanitic to fine-grained groundmass (Fig. 10d). The dike crosscuts a

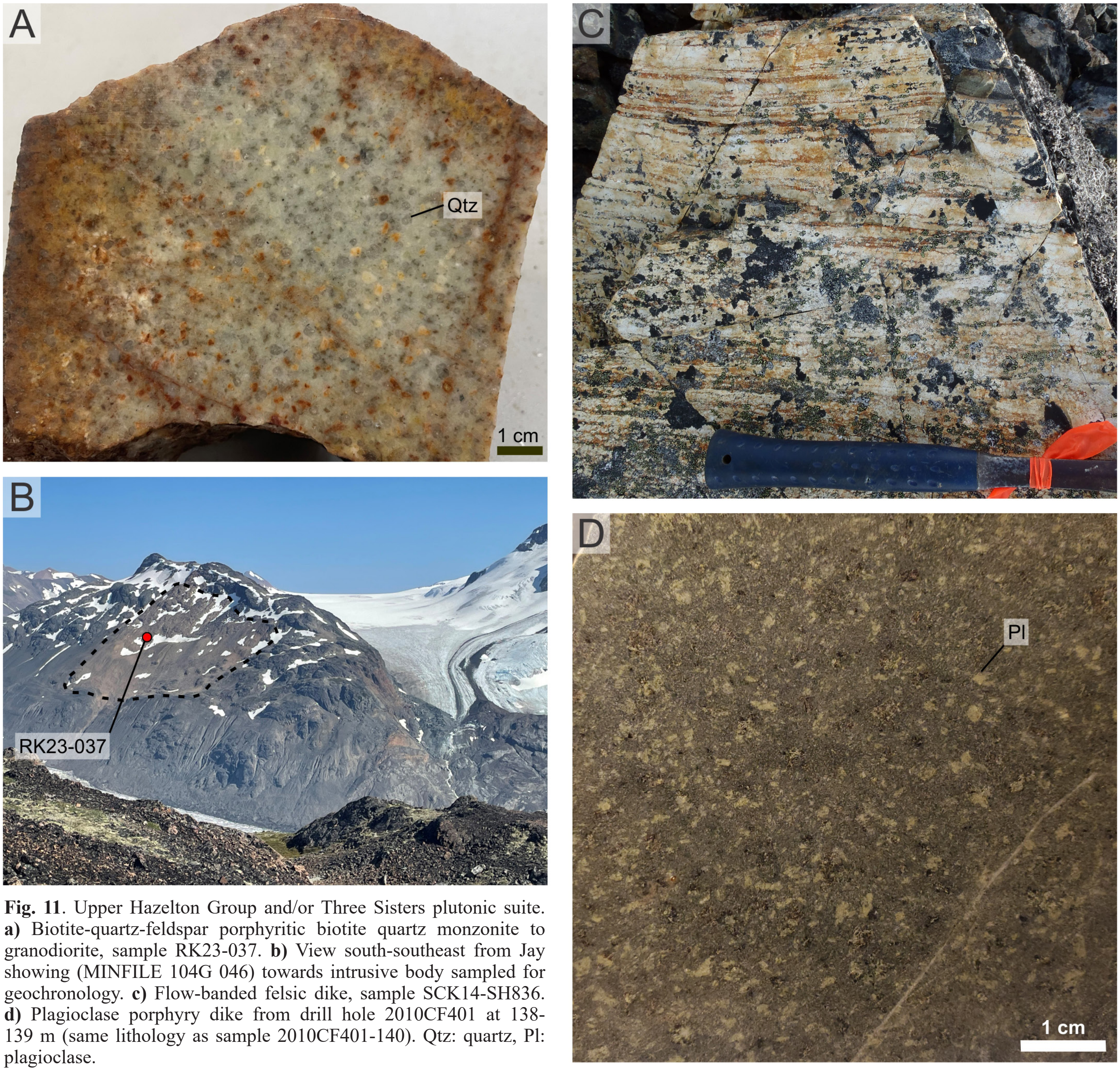

Fig. 11. Upper Hazelton Group and/or Three Sisters plutonic suite. **a)** Biotite-quartz-feldspar porphyritic biotite quartz monzonite to granodiorite, sample RK23-037. **b)** View south-southeast from Jay showing (MINFILE 104G 046) towards intrusive body sampled for geochronology. **c)** Flow-banded felsic dike, sample SCK14-SH836. **d)** Plagioclase porphyry dike from drill hole 2010CF401 at 138-139 m (same lithology as sample 2010CF401-140). Qtz: quartz, Pl: plagioclase.

mineralized hydrothermal breccia body (logging code HBX) of the Paramount zone.

Three zircon grains were analyzed by CA-TIMS. The youngest zircon grain yielded a $^{206}Pb/^{238}U$ date of 178.20 ± 0.40 Ma (Fig. 12d). The mafic composition and fine-grained subvolcanic texture of the dike suggests the magma may not have crystallized zircon, hence the age is interpreted as an igneous crystallization or xenocryst age. Two older grains yielded 221.61 ± 0.43 Ma and 344.00 ± 0.40 Ma dates and are interpreted as xenocrysts.

Although only one late Early Jurassic zircon was recovered from this sample, the lithology and maximum age may suggest a relationship in which the dike acted as a feeder to mafic volcanic rocks in the upper Hazelton Group (Horn Mountain Formation, ca. 185-175 Ma; Brown et al., 1996; van Straaten, 2024).

3.4.4. Sample GJ-14-001

We sampled a quartz syenite dike north-northwest of the LaCasse showing (MINFILE 104G 190). The dike crosscuts equigranular quartz monzodiorite (logging code QMZ; Jutras and Bailey, 2016; Erbalaban, 2023) to granodiorite (logging code GRD) of the Hickman pluton, and crosscuts andesitic dikes (logging code dAN).

Six zircon grains from sample GJ-14-001 analyzed by CA-TIMS yield a weighted mean date of 177.19 ± 0.06 / 0.08 / 0.21 Ma (MSWD = 1.4, probability = 0.22; Fig. 12e), which is interpreted as the igneous crystallization age.

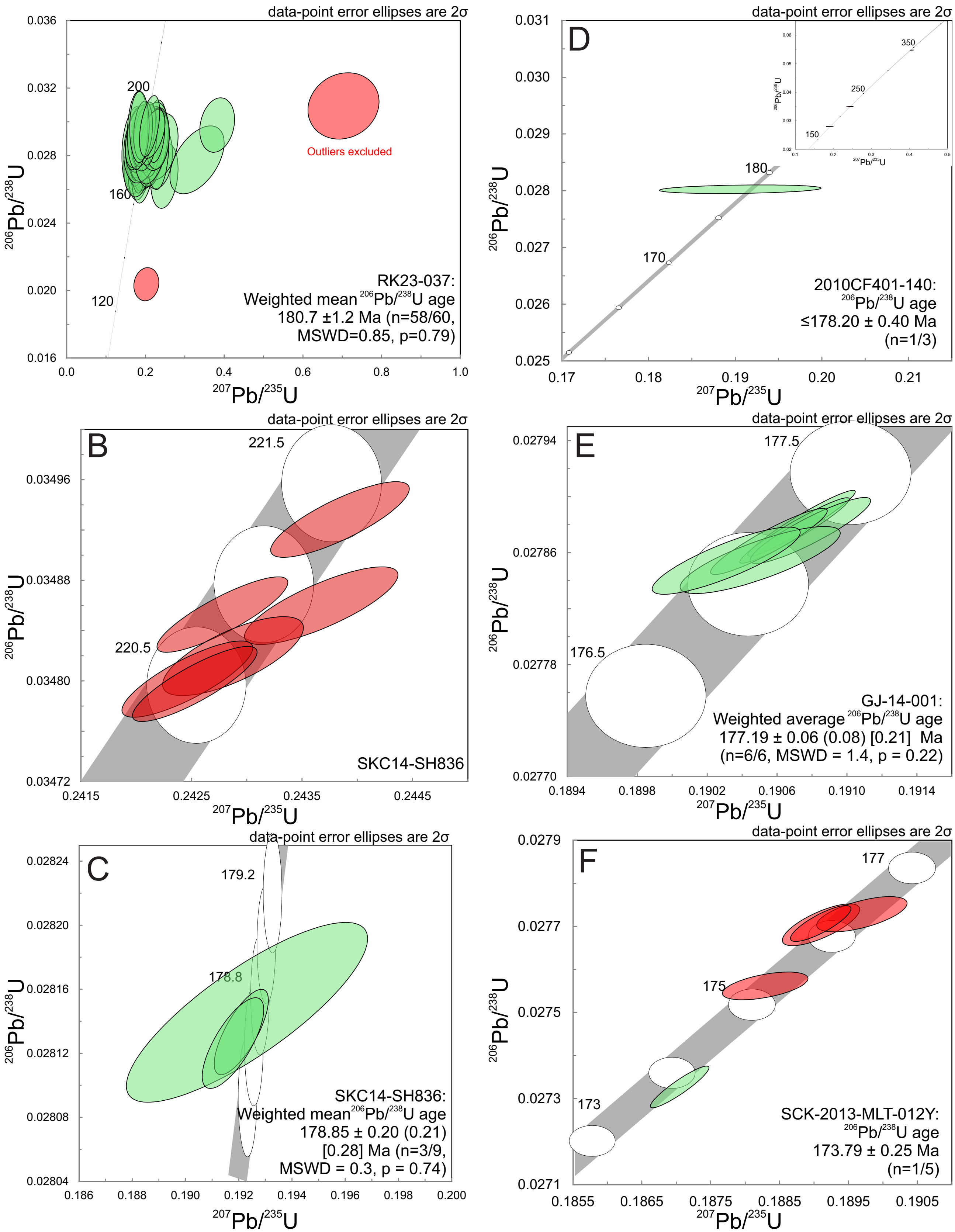

Fig. 12. Upper Hazelton Group and/or Three Sisters plutonic suite. U-Pb concordia diagrams with **a)** LA-ICPMS results from sample RK23-037, **b)** CA-TIMS results from Triassic grains in sample SKC14-SH836, **c)** CA-TIMS results from Jurassic grains in sample SKC14-SH836, **d)** CA-TIMS results for Jurassic grain (inset shows all grains) in sample 2010CF401-140, e) CA-TIMS results from sample GJ-14-001, and **f)** CA-TIMS results from sample SCK-2013-MLT-012Y.

The lithology and age may suggest a relationship in which the dike acted as a feeder to volcanic rocks in the upper Hazelton Group (Horn Mountain Formation, ca. 185-171 Ma; Brown et al., 1996; van Straaten, 2024). Alternatively, the dike may have an affinity with early phases of the Three Sisters plutonic suite (ca. 173-169 Ma; van Straaten et al., 2022 and references therein).

3.4.5. Sample SCK-2013-MLT-012Y

We sampled a pink medium-grained hornblende-bearing biotite syenogranite from the Yehiniko pluton. The sample contains 5% hornblende, 10% biotite (1-2 mm), 20% quartz, 45% K-feldspar, and 20% plagioclase (2-4 mm). The sample is non-magnetic, unaltered and not mineralized.

Five zircon grains were analyzed by CA-TIMS. The youngest zircon grain yielded a $^{206}Pb/^{238}U$ date of 173.79 ± 0.25 Ma (Fig. 12f), which is interpreted as the igneous crystallization age of the Yehiniko pluton. Another grain yielded a $^{206}Pb/^{238}U$ date of 175.27 ± 0.17 Ma, and the three oldest grains yielded a weighted mean $^{206}Pb/^{238}U$ date of 176.23 ± 0.13 Ma (MSWD = 0.61, probability = 0.54). The four oldest grains are interpreted as antecrysts or xenocrysts.

3.5. Unassigned Late Cretaceous plutonic suite

3.5.1. Sample RK23-117

We sampled a fine- to medium-grained, unfoliated, equigranular pyroxene-biotite diorite (Fig. 13) west of Mess Creek (Fig. 1).

Sixty zircon grains were analyzed by LA-ICPMS and yielded a weighted mean $^{206}Pb/^{238}U$ date of 82.62 ± 0.52 Ma (MSWD = 0.49, probability = 1; Fig. 14), which is interpreted as the igneous crystallization age.

The sample was taken from within the northern part of a ~1 km^2 intrusive body previously interpreted as Early Devonian and described as foliated to equigranular green pyroxene quartz diorite and local chlorite schist (Logan et al., 2000). In a traverse across the northwestern part of the intrusive body we observed obscured to sharp and irregular contacts with the surrounding foliated metasedimentary rocks (schists). The intrusion in this area does not appear to be foliated, and foliation in the metasedimentary rocks appears to be truncated by the intrusion.

Fig. 13. Unassigned Late Cretaceous plutonic suite. Fine-grained biotite pyroxene diorite, sample RK23-117. M: mafic mineral, Pl: plagioclase

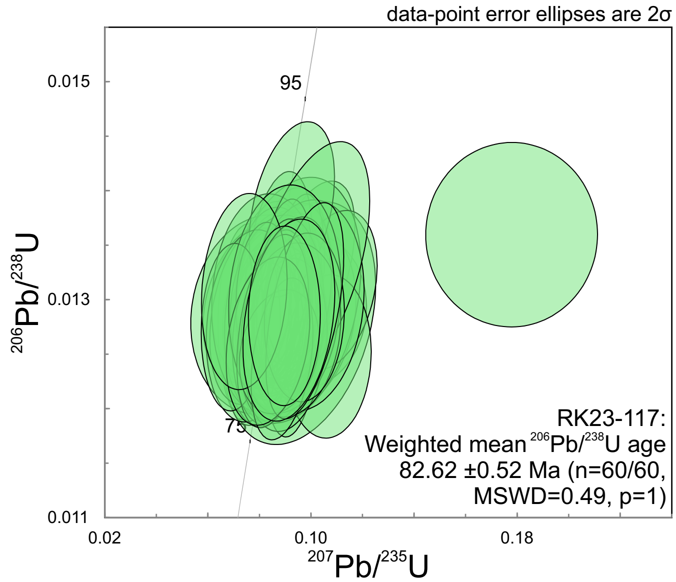

Fig. 14. Unassigned Late Cretaceous plutonic suite. U-Pb concordia diagram with LA-ICPMS results from sample RK23-117.

Acknowledgement

The authors thank Teck Resources Limited and Galore Creek Mining Corporation for permission to publish.

References cited

Black, L.P., Kamo, S.L., Allen, C.M., Davis, D.W., Aleinikoff, J.N., Valley, J.W., Mundil, R., Campbell, I.H., Korsch, R.J., Williams, I.S., and Foudoulis, C., 2004. Improved $^{206}Pb/^{238}U$ microprobe geochronology by the monitoring of a trace-element-related matrix effect; SHRIMP, ID-TIMS, ELA-ICP-MS and oxygen isotope documentation for a series of zircon standards. Chemical Geology 205, 115-140.

Brown, D.A., Greig, C.J., Bevier, M.L., and McClelland, W.C., 1992. U-Pb zircon ages for the Hazelton Group and Cone Mountain and Limpoke plutons, Telegraph Creek map area, northwestern British Columbia: age constraints on volcanism and deformation. In: Radiogenic Age and Isotopic Studies: Report 6, Geological Survey of Canada, Paper 92-2, pp. 153-162.

Brown, D.A., Gunning, M.H., and Greig, C.J., 1996. The Stikine project: Geology of western Telegraph Creek map area, northwestern British Columbia. British Columbia Ministry of Employment and Investment, British Columbia Geological Survey Bulletin 95, 130p.

Campbell, R.W., and van Straaten, B.I., 2025. New data on Late Triassic to late Early Jurassic plutonic suites in the northern Golden Triangle region of northwest British Columbia. In: Geological Fieldwork 2024, British Columbia Ministry of Mining and Critical Minerals, British Columbia Geological Survey Paper 2025-01, pp. 49-72.

Coulson, I.M., Russell, J.K., and Dipple, G.M., 1999. Origins of the Zippa Mountain pluton: a Late Triassic, arc-derived, ultrapotassic magma from the Canadian Cordillera. Canadian Journal of Earth Sciences, 36, 1415-1434.

Crowley, J.L., Schoene, B. and Bowring, S.A., 2007. U-Pb dating of zircon in the Bishop Tuff at the millennial scale. Geology, 35, 1123-1126.

Eggins, S. M., Grün, R., McCulloch, M. T., Pike, A. W., Chappell, J., Kinsley, L., Mortimer, G., Shelley, M., Murray-Wallace, C.V., Spötl, C., and Taylor, L. 2005. In situ U-series dating by laser-ablation multi-collector ICPMS: new prospects for Quaternary

geochronology. Quaternary Science Reviews, 24, 2523-2538.
Enduro Metals Corp., 2021. University study pinpoints Enduro's Burgundy system as Galore Creek suite. News release, January 18, 2021. <https://endurometals.com/university-study-pinpoints-enduros-burgundy-system-as-galore-creek-suite/> Last accessed February 20, 2025.
Erbalaban, G., 2023. 2022 Assessment report on the Schaft Creek porphyry-copper-gold-molybdenum-silver deposit. British Columbia Ministry of Energy and Mines, Assessment Report 40875, 1132 p.
Gerstenberger, H., and Haase, G., 1997. A highly effective emitter substance for mass spectrometric Pb isotopic ratio determinations. Chemical Geology. 136, 309-312.
Jaffey, A.H., Flynn, K.F., Glendenin, L.E., Bentley, W.C., and Essling, A.M., 1971. Precision measurements of half-lives and specific activities of ^{235}U and ^{238}U, Physical Review C, 4, 1889-1906.
Jutras, G., and Bailey, L., 2016. Drilling geological geochemical geophysical report on the Schaft Creek property. British Columbia Ministry of Energy and Mines, Assessment Report 35967, 1345 p.
Kretz, R., 1983. Symbols for rock-forming minerals. American Mineralogist, 68, 227-279.
Krogh, T.E., 1973. A low contamination method for hydrothermal decomposition of zircon and extraction of U and Pb for isotopic age determination. Geochimica et Cosmochimica Acta, 37, 485-494.
Krogh, T.E., 1982. Improved accuracy of U-Pb zircon ages by the creation of more concordant systems using an air abrasion technique. Geochimica et Cosmochimica Acta, 46, 637-649.
Kuiper, Y.D., Murray, D.P., Ellison, S., and Crowley, J.L., 2022. U-Pb detrital zircon analysis of sedimentary rocks of the southeastern New England Avalon terrane in the U.S. Appalachians: Evidence for a separate crustal block. In: Kuiper, Y.D., Murphy, J.B., Nance, R.D., Strachan, R.A., and Thompson, M.D. (Eds), New Developments in the Appalachian-Caledonian-Variscan Orogen. Geological Society of America Special Paper, 554, pp. 93-119. https://doi.org/10.1130/2021.2554(05)
Logan, J.M., and Koyanagi, V.M., 1994. Geology and mineral deposits of the Galore Creek area. British Columbia Ministry of Energy, Mines and Petroleum Resources, British Columbia Geological Survey, Bulletin 92, 102p.
Logan, J.M., and Mihalynuk, M.G., 2014. Tectonic controls on early Mesozoic paired alkaline porphyry deposit belts (Cu-Au ± Ag-Pt-Pd-Mo) within the Canadian Cordillera. Economic Geology, 109, 827-858. https://doi.org/10.2113/econgeo.109.4.827
Logan, J.M., Drobe, J.R., and McClelland, W.C., 2000. Geology of the Forrest Kerr-Mess Creek area, northwestern British Columbia. British Columbia Ministry of Energy and Mines, British Columbia Geological Survey Bulletin, 104, 132p.
Ludwig, K.R., 1980. Calculation of uncertainties of U-Pb isotopic data. Earth and Planetary Science Letters, 46, 212-220.
Ludwig, K.R., 2003. User's manual for Isoplot 3.00: A geochronological toolkit for Microsoft Excel. Berkeley Geochronology Center, University of California at Berkeley, 70 p.
Mattinson, J.M., 2005. Zircon U-Pb chemical abrasion ("CA-TIMS") method: Combined annealing and multi-step partial dissolution analysis for improved precision and accuracy of zircon ages. Chemical Geology, 220, 47-66.
Mortensen, J.K., Ghosh, D., and Ferri, F., 1995. U-Pb age constraints of intrusive rocks associated with copper-gold porphyry deposits in the Canadian Cordillera. In: Schroeter, T. G. (Ed.), Porphyry Deposits of the Northwestern Cordillera of North America. Canadian Institute of Mining and Metallurgy Special Volume 46, pp. 142-158.
Mundil, R., Ludwig, K. R., Metcalfe, I., and Renne, P. R., 2004. Age and timing of the Permian mass extinctions: U/Pb dating of closed-system zircons, Science, 305, 1760-1763.
Parrish, R.R., Roddick, J.C., Loveridge, W.D., and Sullivan, R.W., 1987. Uranium-lead analytical techniques at the geochronology laboratory. In: Radiogenic Age and Isotopic Studies: Report 1, Geological Survey of Canada, Paper 87-2, pp. 3-7.
Paton, C., Hellstrom, J., Paul, B., Woodhead, J., and Hergt, J., 2011. Iolite: Freeware for the visualisation and processing of mass spectrometric data. Journal of Analytical Atomic Spectrometry, 26 (12), 2508-2518.
Prince, J., 2020. 2019 drilling, geological mapping and aerial survey assessment report on the Galore Creek project. British Columbia Ministry of Energy, Mines and Petroleum Resources, Assessment Report 39156, 48p.
Schmitz, M.D., and Schoene, B., 2007. Derivation of isotope ratios, errors, and error correlations for U-Pb geochronology using ^{205}Pb-^{235}U-(^{233}U)-spiked isotope dilution thermal ionization mass spectrometric data. Geochemistry, Geophysics, Geosystems, 8, article Q08006. https://doi.org/10.1029/2006GC001492
Scoates, J.S., and Friedman, R.M., 2008. Precise age of the platiniferous Merensky reef, Bushveld Complex, South Africa, by the U-Pb zircon chemical abrasion ID-TIMS technique, Economic Geology, 103, 465-471.
Sláma, J., Košler, J, Condon, D.J., Crowley, J.L., Gerdes, A., Hanchar, J.M., Horstwood, M.S.A., Morris, G.A., Nasdala, L., Norberg, N., Schaltegger, U., Schoene, B. Tubrett, M.N., and Whitehouse, M.J., 2008. Plešovice zircon - A new natural reference material for U-Pb and Hf isotopic microanalysis. Chemical Geology, 249, 1-35.
Stacey, J.S., and Kramers, J.D., 1975. Approximation of terrestrial lead isotopic evolution by a two-stage model. Earth and Planetary Science Letters, 26, 207-221.
Thirlwall, M.F., 2000. Inter-laboratory and other errors in Pb isotope analyses investigated using a ^{207}Pb-^{204}Pb double spike. Chemical Geology, 163, 299-322.
Todt, W., Cliff, R., Hanser, A., and Hofman, A.W., 1984. ^{202}Pb + ^{205}Pb double spike for lead isotopic analyses. Terra Cognita, 4, 209.
van Straaten, B.I., 2024. Upper Hazelton Group stratigraphy along the Stikine arch, northwestern British Columbia. In: Geological Fieldwork 2023, British Columbia Ministry of Energy, Mines and Low Carbon Innovation, British Columbia Geological Survey Paper 2024-01, pp. 149-177.
van Straaten, B.I., Logan, J.M., Nelson, J.L., Moynihan, D.P., Diakow, L.J., Gibson, R., Bichlmaier, S.J., Wearmouth, C.D., Friedman, R.M., Golding, M.L., Miller, E.A., and Poulton, T.P., 2022. Bedrock geology of the Dease Lake area. British Columbia Ministry of Energy, Mines and Low Carbon Innovation, British Columbia Geological Survey Geoscience Map 2022-01, 1:100,000 scale.
Vermeesch, P., 2018. IsoplotR: A free and open toolbox for geochronology. Geoscience Frontiers, 9, 1479-1493. https://doi.org/10.1016/j.gsf.2018.04.001
Watson, E.B., Wark, D.A., and Thomas, J.B., 2006. Crystallization thermometers for zircon and rutile. Contributions to Mineralogy and Petrology, 151, 413-433.
Wiedenbeck, M., Alle, P., Corfu, F., Griffin, W.L., Meier, M., Oberli, F., von Quadt, A., Roddick, J.C., and Spiegel, W., 1995. Three natural zircon standards for U-Th-Pb, Lu-Hf, trace element and REE analyses. Geostandards Newsletter, 19, 1-23.
Wiedenbeck, M., Hanchar, J.M., Peck, W.H., Sylvester, P., Valley, J., Whitehouse, M., Kronz, A., Morishita, Y., Nasdala, L., Fiebig, J., Franchi, I., Girard, J.-P., Greenwood, R.C., Hinton, R., Kita, N., Mason, P.R.D., Norman, M., Ogasawara, M., Piccoli, P.M., Rhede, D., Satoh, H., Schulz-Dobrick, B., Skår, O., Spicuzza, M., Terada, K., Tindle, A., Togashi, S., Vennemann, T., Xie, Q., and Zheng, Y.-F., 2004. Further characterisation of the 91500 zircon crystal. Geostandards and Geoanalytical Research, 28, 9-39. https://doi.org/10.1111/j.1751-908X.2004.tb01041.x

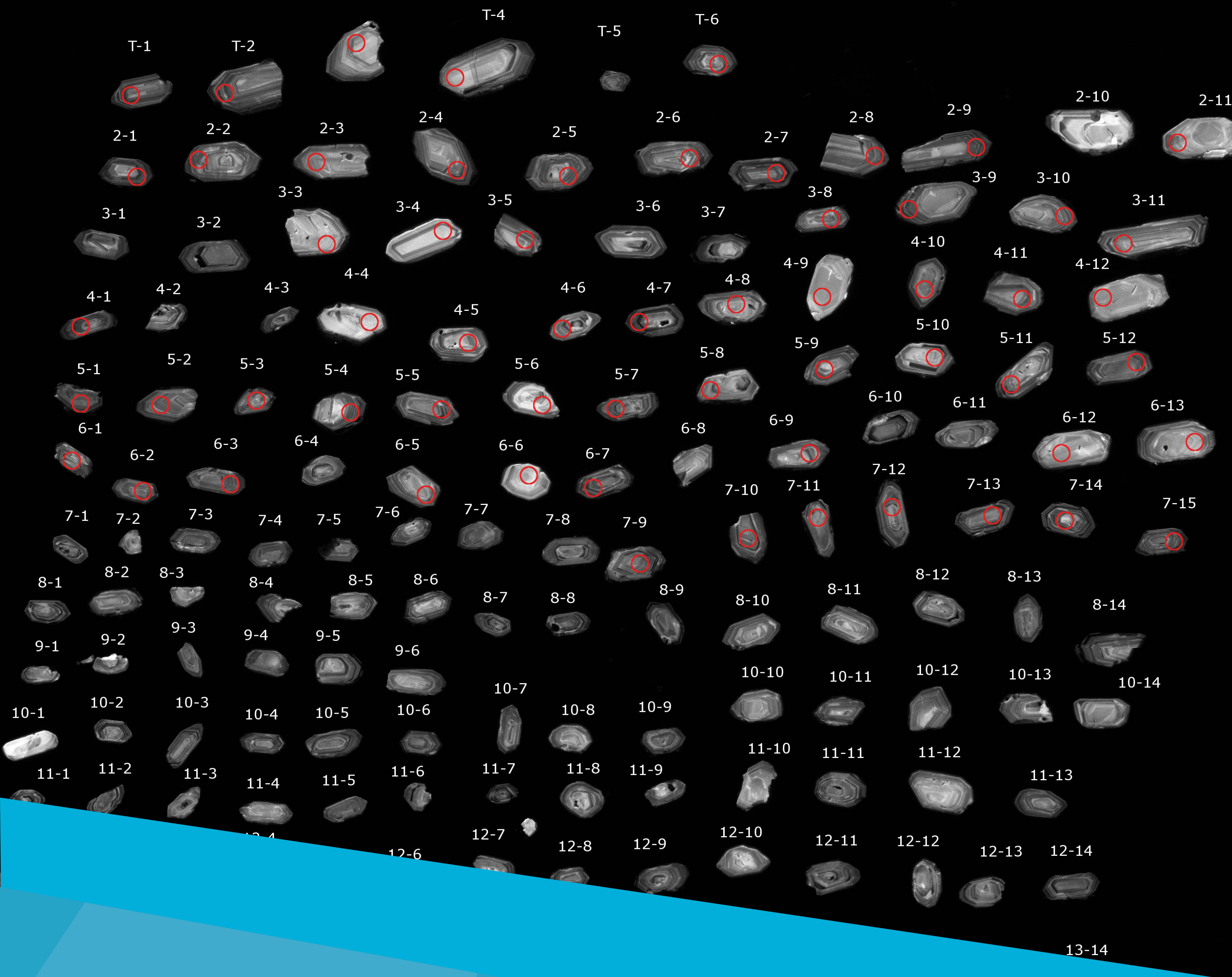

BRITISH COLUMBIA

Ministry of Mining and Critical Minerals

BRITISH COLUMBIA GEOLOGICAL SURVEY est. 1895